AN ON-CHIP ELECTRICALLY SMALL ULTRA-WIDEBAND ANTENNA IN CMOS

by

William Che Knisely

A thesis submitted to the
Faculty of Graduate and Postdoctoral Affairs
in partial fulfillment of the requirements for the degree of

Master of Applied Science in Electrical and Computer Engineering

Ottawa-Carleton Institute for Electrical Engineering
Department of Electronics
Faculty of Engineering
Carleton University
Ottawa, Canada

September, 2010

Your file Votre référence
ISBN: 978-0-494-71512-3
Our file Notre référence
ISBN: 978-0-494-71512-3

Abstract

Recent allocation of the Ultra WideBand (UWB) 3.1 to 10.6 GHz frequency spectrum for unlicensed use has opened many new opportunities for radio communications. Providing unique advantages as well as interesting design challenges makes UWB an attractive technology to pursue. Furthering the challenge is the desire to monolithically integrate an UWB radio with an antenna. Such a feat would reduce manufacturing complexity, while maintaining a high level of cost effectiveness. With these two technologies in mind, as well as traditional methods, design considerations for the development of an on-chip ultra wideband antenna in CMOS are discussed. After a review of current UWB antennas, an electrically small square loop radiator integrated in a 0.13 μm CMOS process is proposed for use as an UWB antenna. An UWB LNA and pulse generator are monolithically included with the antenna. Simulation results of this antenna show it to perform as expected, having a relatively constant, but poor return loss of less than 1 dB, an omnidirectional radiation pattern, low dispersion, and a maximum gain ranging from -25 dBi to -35 dBi over the UWB spectrum. Due to complications with the on-chip circuitry, measurements are unable to confirm the radiation patterns and transient response of the antenna. Despite this, measurements show the maximum gain is in good agreement with simulation over the entire band, while the return loss is less than 10 dB, but shows multiple unexpected resonances. Phase response of the antenna was linear with an R^2 value of 0.99, indicating the antenna may be a good device for use with impulse radios. Although the results are somewhat inconclusive, data does indicate the antenna is still potentially a viable candidate for use with UWB.

Acknowledgements

I would like to thank my supervisor, Calvin Plett, who has been only supportive, assistive, and patient beyond requirement. Also, I thank the many students, faculty, and staff of the Department of Electronics at Carleton University for their assistance, support, and for this opportunity to learn and grow. Although the credit may be solitary, this thesis was only possible by the actions of a group effort.

The financial support of Carleton University and Natural Sciences and Engineering Research Council of Canada (NSERC) is gratefully acknowledged.

Finally, I wish to thank my spouse for her constant support and encouragement during the long hours I spent working towards this milestone in my life and career.

Table of Contents

List of Tables

List of Figures

List of Acronyms

ADL – Artificial Dielectric Layer
CMOS – Complementary Metal-Oxide-Semiconductor
EIRP – Equivalent Isotropically Radiated Power
FCC – Federal Communications Commission (United States)
FI – Frequency Independent
GSG – Ground-Signal-Ground
HFSS – High Frequency Structure Simulator (Ansoft)
HPBW – Half Power Beamwidth
IC – Integrated Circuit
IEEE – Institute of Electrical and Electronics Engineers
UWB-IR – Ultra Wideband Impulse Radio
LNA – Low Noise Amplifier
MOS – Metal-Oxide-Semiconductor
OFDM – Orthogonal Frequency-Division Multiplexing
PCB – Printed Circuit Board
PSD – Power Spectral Density
RF – Radio Frequency
Rx – Receiver or Reception
SC – Self Complementary
TW – Traveling Wave
Tx – Transmitter or Transmission
USA – United States of America
UWB – Ultra-Wideband
VCO – Voltage Controlled Oscillator
VLSI – Very Large Scale Integration
VSWR – Voltage Standing Wave Ratio
WLAN – Wireless Local Area Network

Chapter 1: Introduction

The "era of long-distance radiocommunications was born" in 1901, ushered in by the first cross Atlantic transmission of an electromagnetic signal [**1**]. Pioneered by Guglielmo Marconi, this accomplishment led to the first commercial trans-Atlantic radio telegraphy service in 1907 [**1**] and the awarding of a Nobel Prize in 1909 [**2**], recognizing wireless communications as both an industrial and academic success from its inception.

Modern wireless communications have evolved greatly beyond the first telegraphy systems, in both technical complexity and application. Improvements in coding and modulation techniques have increased efficiency, allowing greater amounts of information to be transmitted over a given bandwidth. Advancements in electrical circuitry have allowed devices to become smaller and smaller, with greater complexity, yet facilitate mass production while remaining cost effective. Modern wireless communication devices have become compact, generally affordable, and more powerful with each generation of development, leading to a near ubiquitous presence.

A key component to the circuitry of any radio is the antenna. This thesis looks to investigate the development of an antenna using the combination of two technologies: Complementary Metal-Oxide-Semiconductor (CMOS) Integrated Circuits (ICs) and Ultra-Wideband (UWB) pulsed signal generation. Although neither of these areas are considered new, the combination of each to integrate a wideband antenna has only recently been considered.

1.1 Ultra-Wideband Communications

In February, 2002 the Federal Communications Commission (FCC) of the United States of America (USA) authorized the unlicensed use of UWB emissions in the 3.1 to 10.6 GHz range [**3**]. This change has led to an enthusiastic renewal of interest in UWB radio as it can be favourable for several reasons, including low power high data rate transmissions, accurate ranging, interference rejection, and coexistence with narrow bandwidth systems [**4**].

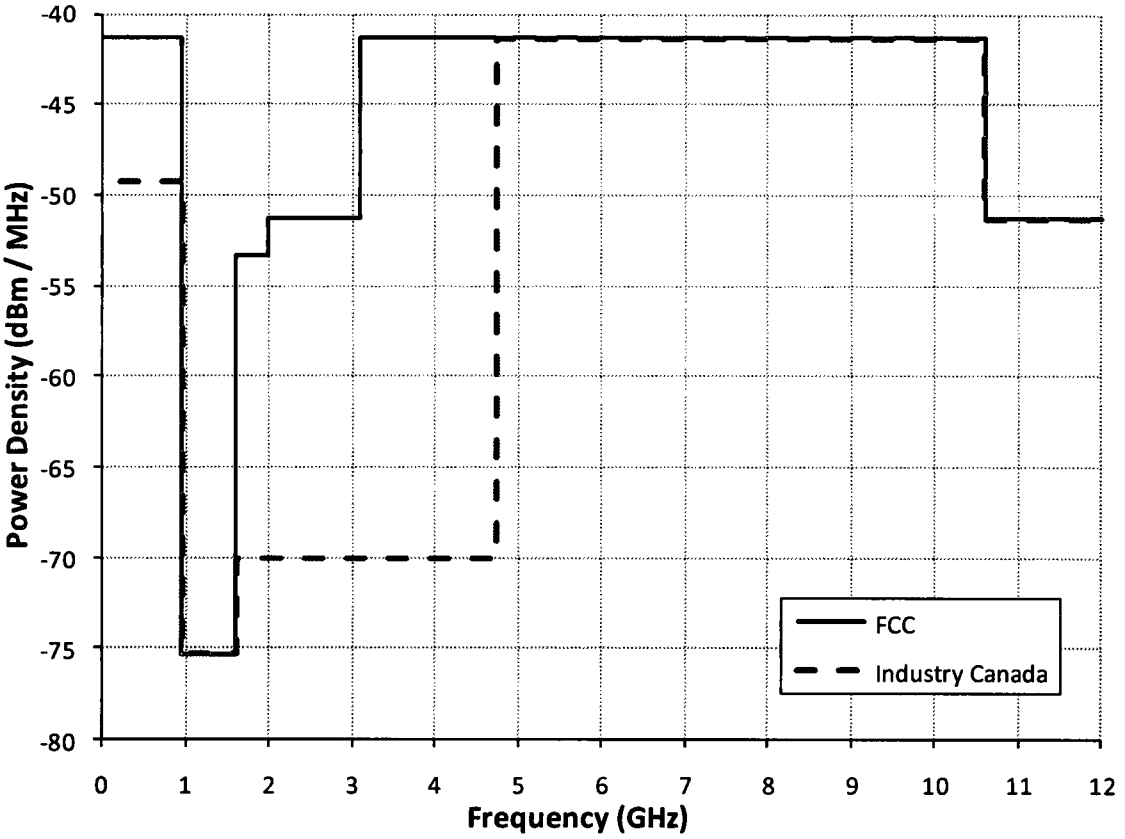

Figure 1-1. FCC and Industry Canada spectral mask for unlicensed indoor UWB emissions.

Utilizing such a large frequency band, UWB operates at a relatively low Power Spectral Density (PSD) of 41.3 dBm/MHz. This specification is required to avoid possible

interference with narrow band signals that may also be present in the UWB range. Additionally, greater restrictions are present outside the 3.1 to 10.6 GHz range in the USA [**5**] and the 4.75 to 10.6 GHz range in Canada [**6**]. The FCC's and Industry Canada's spectral requirements for indoor UWB emissions are shown in Figure 1-1.

The specifications lead to an interesting and unique challenge for UWB design, as not only is wideband operation required, but also a well defined spectral shape. This has a large impact on a broad selection of research, including signal generation, transmission, propagation, processing, and system engineering. Even with these challenges, many opportunities for novel and effective solutions to the design problems featured in UWB are permitted, three promising areas of application already being identified: short range high data rate communications, low data rate sensor networks with ranging and geo-location, and high resolution radar systems [**4**].

Antenna design is substantially impacted by UWB. Maintaining a reasonable efficiency and impedance match over such a large bandwidth becomes difficult, while transient response, typically not a concern, becomes an important issue [**7**] [**8**]. UWB antenna development is not as straightforward as narrowband antenna development, which is relatively mature and well understood. Given the potential benefit to applications, but the complexities added by UWB, design of an UWB antenna piques a great interest [**9**].

1.2 On-Chip Antennas

Integration, in electronics and electrical engineering, refers to the monolithic development of circuitry in a single medium, typically a semiconductor. This amalgamation of electrical components is motivated by the desire to simplify construction, lower costs, and reduce the size of electronic circuits, goals that have been amazingly successful [**10**]. The pervasive presence of electronics owes its existence to the integration of just about every circuit necessary to create such devices, in particular the analog circuits necessary for radios [**11**].

Despite its great success, integration is not a perfect art. Strongly linked to the material science of semiconductors [**12**], the performance of ICs has boundaries limited by the characteristics of the semiconductor in which the circuits are integrated. Additionally, the ability, or lack of, to physically manipulate these materials into the forms required can limit performance. This leads to incongruous ICs, not all components being integrated into a single monolithic circuit for performance reasons, and stimulates research focused on the development of truly monolithic electronic devices.

As a key component of any radio, antennas are traditionally found 'off-chip' due to two main factors: size and material properties. It is common that at least one dimension of a resonant antenna's size is on the order of one wavelength of the frequency of operation, which can be several orders of magnitude greater than the IC itself. Thus, for many applications, to place an antenna 'on-chip' requires special consideration and the use of miniaturization techniques. Additionally, the electrical

characteristics, such as substrate losses and surface wave effects, of the IC can negatively impact an integrated antenna's performance. These factors, too, require special design considerations.

Given the great advantages that integration brings to any electrical circuit, it becomes obvious why having an antenna on-chip would be favourable, despite the challenges presented. With a successful design, incorporating an antenna into an IC would lower production costs and complexity, removing the need for external transmission line connections and sophisticated packaging. Additionally, an opportunity is presented to create a multi-purpose element: an antenna that not only functions as a radiator, but also as an intrinsic component of the circuit itself, able to provide better matching and more robust capabilities. [**13**]

1.3 Thesis Outline

After first discussing the motivation behind developing an UWB CMOS integrated antenna in Chapter 1, this report reviews general antenna design considerations in Chapter 2. The review includes a look at fundamental antenna design parameters and characteristics as well as the special exigencies required by UWB and on-chip CMOS integration. The review is followed by a survey of current UWB antennas, on-chip CMOS antennas, and UWB on-chip antennas, giving a brief summary of each in Chapter 3. In Chapter 4, the on-chip UWB loop antenna that was developed for this thesis is presented. A discussion of the antenna's design, simulation, and measurement is followed by a listing of the results. Finally, in Chapter 5, concluding remarks are made along with a discussion of the future work required.

Chapter 2: Fundamental, UWB, and CMOS Antenna Design

The project for this thesis centers on the development of an antenna incorporating two technologies, UWB pulsed signals and CMOS ICs, for use in a low cost, self contained transceiver. In addition to typical design concerns, special considerations necessary to implement an antenna in CMOS using UWB must be observed. The various technological aspects of the project are discussed below, highlighting these areas of interest.

2.1 Fundamental Antenna Design

Antennas are commonly the first and last component in the signal path of a transceiver. As such they take an interesting and unique position in the operation of the radio: unlike the other components, antennas must couple with free-space as well as the radio's circuitry. This means that antennas require special design considerations as well as unique characterisations.

The theory of antennas deals mainly with calculations regarding the radiation, into free space, of electromagnetic fields from a conducting structure and the propagation of those fields from and to another conducting structure. The various characteristics of antennas are derived from Maxwell's Equations [**14**] and are parameterized as laid out in the IEEE Standard Definitions of Terms for Antennas [**15**], some of which are discussed below.

2.1.1 Near and Far Field

The volume surrounding an antenna is broken into two areas: near field and far field. For the most part, the far field is taken as the more significant as antenna operation is generally at large distances. The following parameters are usually determined for the far field case. Even so, in cases where the transmitting and receiving antennas may be close it is important to determine if near field affects may be present. To this end the two areas are given as follows.

The far field is defined as the region where the radiated angular field distribution is effectively independent of the distance, r, from the antenna. In free space, this distance is estimated as:

$$r > \frac{2a^2}{\lambda}, \tag{2.1}$$

where a is the maximum overall dimension of the antenna and λ is the wavelength. This is commonly only valid for cases where a is large compared to λ, otherwise the more general condition is for a distance where $r \gg \lambda$. It can be shown that, in the far field, the electromagnetic fields are transverse, always approximated by plane waves in a local area, and the power is real, being completely dissipative.

The near field is found between the antenna and the far field and is broken into two parts: radiating and reactive. The reactive portion is found near the antenna, the volume for which is estimated as $r < \lambda/2\pi$ for very short dipole, or similar, antennas. Within the reactive region, the power is mainly imaginary and thus implies stored

energy. The radiating region falls between the reactive region and the far field, having an angular field distribution that is dependent on the distance, r, from the antenna. Together, with the power being complex, this makes the electromagnetic fields in the near field non-intuitive and difficult to predict. Antennas that are small compared to the wavelength may not exhibit a radiating near field.

2.1.2 Reciprocity

Reciprocity refers to the characteristics of an antenna remaining unchanged whether that antenna is used as a transmitter or receiver. The transmitting radiation patterns of a given antenna are identical to the receiving radiation patterns, as are the input impedances and other parameters. This has practical application in that only one design or measurement (transmit or receive) is necessary to develop or characterize an antenna.

It is important to note that reciprocity is not applicable in all cases. It is generally true for narrow band passive antennas that the frequency domain transmit and receive characteristics will be the same, but it is common for UWB antennas, as well as some other antennas, such as ferrite core antennas, to have differing time domain transmit and receive characteristics. For example, it is typical for some UWB antennas to act as a differentiator, displaying a signal at the receiver that is the differential of that which was transmitted.

2.1.3 Radiation Intensity, Directivity, and Isotropic Antennas

The main purpose of an antenna is to direct energy through space. Thus it is important to ascertain how an antenna prefers to guide energy to or from one direction over another. This is accomplished using radiation intensity and directivity.

The total power radiated by an antenna is given by:

$$P_r = \frac{1}{2} Re\left\{\iint (\mathbf{E} \times \mathbf{H}^*) \cdot d\mathbf{s}\right\}, \tag{2.2}$$

where **E** is the electric field and **H** is the magnetic field radiated and the integral is over a surface in the far field surrounding the antenna. For simplicity the surface is typically taken as a sphere. Recalling the electromagnetic fields are localized TEM plane waves in the far field:

$$P_r = \frac{1}{2} Re\left\{\iint (E_\theta H_\varphi^* - E_\varphi H_\theta^*) r^2 d\Omega\right\}, \tag{2.3}$$

where $d\Omega = Sin\,\theta\, d\theta\, d\varphi$, an element of a solid angle. It then becomes opportune to define the radiation intensity of the antenna as:

$$U(\theta,\varphi) = \frac{1}{2} Re\{(\mathbf{E} \times \mathbf{H}^*) r^2\}, \tag{2.4}$$

which is the power radiated, in a given direction, (θ, φ), per unit solid angle in units of watts per square radian.

Given the radiation intensity, it becomes relatively straightforward to describe the directivity of an antenna as:

$$D(\theta,\varphi) = \frac{U(\theta,\varphi)}{U_{ave}}, \tag{2.5}$$

the ratio of the radiation intensity in a given direction to the average radiation intensity from all directions. The average radiation intensity is simply:

$$U_{ave} = \frac{P_r}{4\pi}. \tag{2.6}$$

Maximum directivity, the directivity in the direction of maximum radiation intensity, is commonly implied using D without θ and φ. Directivity is reciprocal.

To further illustrate the concept of directivity, it is convenient to imagine a lossless antenna, called an isotropic radiator, for which the radiation intensity is equal in all directions. Generally, an equivalent isotropic radiator emits the same total power as supplied to an antenna. Thus an isotropic radiator has constant radiation intensity, U_{ave}, and a directivity of 1. Such an antenna does not practically exist, but it is a useful conceptual reference for highlighting the directive properties of an antenna.

2.1.4 Radiation Efficiency and Gain

The power accepted into the antenna is not equal to the power radiated due to loss effects in the antenna. Thus the antenna has a radiation efficiency given by:

$$e = \frac{P_r}{P_{in}}; 0 \leq e \leq 1. \tag{2.7}$$

Radiation efficiency does not include losses from polarization or impedance mismatches. Combining equations (2.5), (2.6), and (2.7), the directivity of an antenna can then be expressed:

$$D(\theta,\varphi) = \frac{4\pi U(\theta,\varphi)}{eP_{in}}. \tag{2.8}$$

The gain of an antenna, for a given direction, is defined as the ratio of the radiation intensity of the antenna to the radiation intensity of an equivalent isotropic radiator or:

$$G(\theta,\varphi) = \frac{4\pi U(\theta,\varphi)}{P_{in}}. \tag{2.9}$$

From equations (2.8) and (2.9) it is seen:

$$G(\theta,\varphi) = eD(\theta,\varphi) \tag{2.10}$$

Thus it is noted that the gain of antenna is a directional characteristic of the antenna and proportional to the directivity by the radiation efficiency. Similar to directivity, maximum gain, the gain in the direction of maximum directivity, is commonly implied using G without θ and φ. It is also common to express gain in decibels, denoted dBi to indicate it is relative to an isotropic radiator.

2.1.5 Equivalent Isotropically Radiated Power

Equivalent Isotropically Radiated Power (EIRP) is the radiated power an isotropic radiator would emit to produce the same radiation intensity as that of an antenna in a given direction. This is expressed by:

$$\text{EIRP} = P_{in} G(\theta, \varphi). \tag{2.11}$$

Since EIRP includes gain and losses between the circuitry and the antenna, it is a convenient parameter to use when comparing various antennas. EIRP is typically implied to be in the direction of maximum gain and is expressed in dBi.

2.1.6 Antenna Impedance, Matching, and Bandwidth

The impedance of an antenna is the impedance measured at the terminals of the antenna and is generally complex. Note that, due to reciprocity, the impedance of an antenna is referred to as input impedance despite the antenna's use as a transmitter or receiver.

Input impedance is denoted:

$$Z_{in} = R_{in} + jX_{in}. \tag{2.12}$$

The reactance of the antenna, X_{in}, signifies the electromagnetic energy stored in the near field. This corresponds to the large imaginary part of the electromagnetic fields near the antenna as discussed in section 2.1.1. Generally, electrically small antennas, defined as antennas for which $D \ll \lambda$, have large reactive input impedances.

The resistance, R_{in}, arises from the power dissipated in the antenna, which includes radiated power and ohmic losses. The power dissipated by the antenna is then:

$$P_{in} = P_r + P_\Omega = \frac{1}{2} R_{in} |I_{in}|^2, \tag{2.13}$$

where I_{in} is the input current and P_Ω is the power lost to ohmic effects. From equation (2.13) it is noted:

$$R_{in} = R_r + R_\Omega, \tag{2.14}$$

where R_Ω is the resistance due to ohmic losses and R_r is called the radiation resistance, corresponding to the power radiated and is referred to the input.

With the above definitions and equation (2.7), an alternative expression for radiation efficiency can be given as:

$$e = \frac{R_r}{R_r + R_\Omega}, \tag{2.15}$$

which is a convenient when designing an antenna as ohmic resistances are relatively easy to determine.

To ensure maximum power is transferred to or from an antenna, complex conjugate matching must be used:

$$Z_x = Z_{in}^*, \tag{2.16}$$

where Z_x is the input/output impedance of the circuitry connected to the antenna. In general, a matching network is needed to accomplish this, although it is possible to design circuits that are intrinsically matched to the antenna.

Mismatches between the circuit of the radio and the antenna can be expressed using transmission line theory [**16**]. In the transmitting case, the reflection coefficient, Γ, is defined as the ratio between the voltage wave reflected back to the circuitry, V^-, to the voltage wave incident on the antenna's terminals, V^+. The reflection coefficient can be expressed as:

$$\Gamma = \frac{V^-}{V^+} = \frac{Z_{in} - Z_x}{Z_{in} + Z_x}. \tag{2.17}$$

It is also of interest to note that the reflection coefficient is also the S_{11} parameter of the scattering matrix.

It can then be shown that the power accepted by the antenna is:

$$P_{in} = P_i(1 - |\Gamma|^2), \tag{2.18}$$

where P_i is the power incident on the antenna's terminals. The term $(1 - |\Gamma|^2)$ is called the impedance mismatch factor, denoted q, while the term $|\Gamma|^2$ is called return loss, expressed in decibels as:

$$RL = -20\text{Log}|\Gamma|, \tag{2.19}$$

and represents the "loss" of the reflected power. Note, it is common to plot return loss as its negative.

Another convenient measure of impedance mismatch is the Voltage Standing Wave Ratio (VSWR). This is a measure of the ratio of the maximum to the minimum voltage of the standing wave that arises due to the reflected voltage wave. This is given as:

$$VSWR = \frac{V_{max}}{V_{min}} = \frac{1 + |\Gamma|}{1 - |\Gamma|}. \tag{2.20}$$

The bandwidth of an antenna is specified as the frequency range over which a given characteristic of the antenna conforms to some specification. Typically, less than 10% reflected power is chosen as the criterion, which corresponds to $\Gamma = 0.3162$. This is equivalent to RL > 10dB, typically called the -10 dB bandwidth, and VSWR < 1.92, although this is usually rounded to VSWR < 2.

The fractional bandwidth of an antenna is given as:

$$B = \frac{f_H - f_L}{f_c}, \tag{2.21}$$

where f_H and f_L are the high and low frequency boundaries of the bandwidth defined above and f_c is the center frequency given by $(f_H + f_L)/2$.

2.1.7 Antenna Effective Aperture

The effective aperture or effective area of an antenna is a measure of its ability to convert power incident on the antenna to power available at the terminals of the antenna. It is denoted by:

$$A_e = \frac{\lambda^2}{4\pi} G. \tag{2.22}$$

Effective aperture is a convenient parameter when considering the receiving antenna in an antenna system.

2.1.8 Polarization

The polarization of an antenna is the polarization of the electric far field transmitted by the antenna in a given direction. Antenna polarization, in general, is elliptical with special cases where the polarization is circular and linear. Polarization is reciprocal.

Polarization can affect the power transferred between antennas. Maximum power transfer for a given direction occurs when two antennas, receiving and transmitting, are said to have a polarization match. This occurs when, in the same direction, the receiving antenna has the same polarization as the transmitting antenna. The power received will be reduced if a polarization mismatch is present. To gauge the mismatch, the polarization efficiency, p, is defined as the ratio of the power received in a given direction by an antenna from a transmitting antenna of arbitrary polarization

to that of the power that would be received had the antennas been polarization matched in the same direction.

2.1.9 Radiation Pattern

A radiation pattern of an antenna is a spatial mapping describing, either graphically or mathematically, a given characteristic of the electromagnetic field radiated by the antenna. Typical characteristics used are power flux density, radiation intensity, directivity, phase, polarization, and field strength [**15**]. For example, the radiation intensity pattern for an isotropic antenna would appear as a sphere.

Radiation patterns are normally shown graphically and, although 3 dimensional (3D), 2 dimensional (2D) cuts are common, used to highlight specific features of the antenna, such as maximum gain in particular planes. For linearly polarized antennas, typical cut planes are the E-plane and H-plane. The E-plane contains both the electric field vector and the direction of maximum radiation intensity, while the H-plane contains both the magnetic field vector and the direction of maximum radiation intensity. The E-pane and H-plane are orthogonal in the far field. Elevation and azimuth are also common cut planes, where azimuth is parallel to the earth's surface (XY plane) and elevation is perpendicular (YZ plane).

Depending on application it may be desirable to have an antenna with a specific type of radiation pattern. An omnidirectional radiation pattern is one type in which the pattern is mostly a constant value or non-directional in a given plane and directional in the orthogonal plane. An isotropic radiator is the ideal omnidirectional antenna,

although it cannot be realized. Real antennas are always directional in at least one plane. Omnidirectional antennas are used in applications in which the direction of the signal transmission is unknown. An example of an omnidirectional radiation pattern is shown in Figure 2-1.

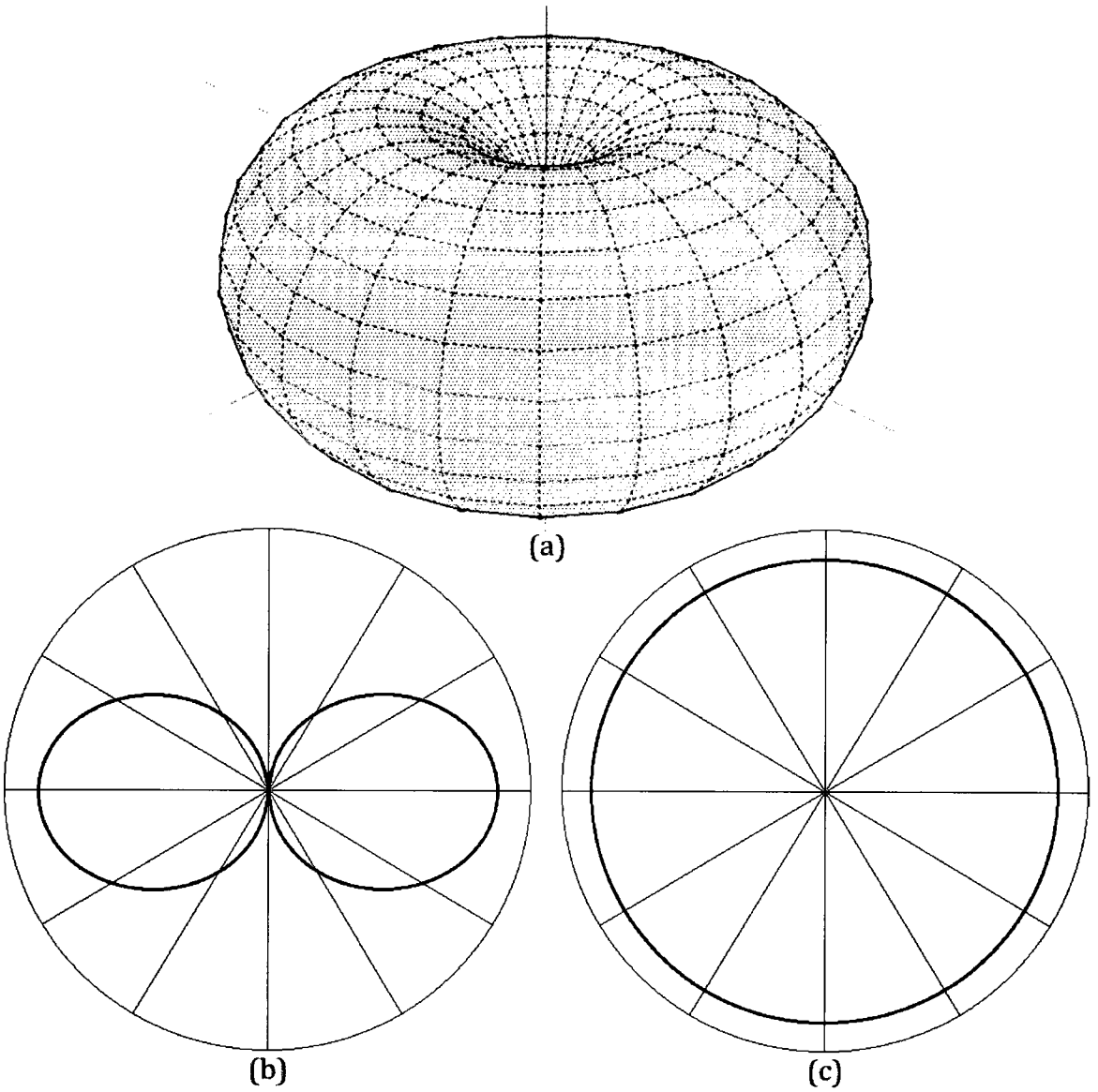

Figure 2-1. Radiation pattern of an omnidirectional dipole antenna: (a) 3D polar plot, (b) E-Plane polar plot (directional), (c) H-Plane polar plot (non-directional).

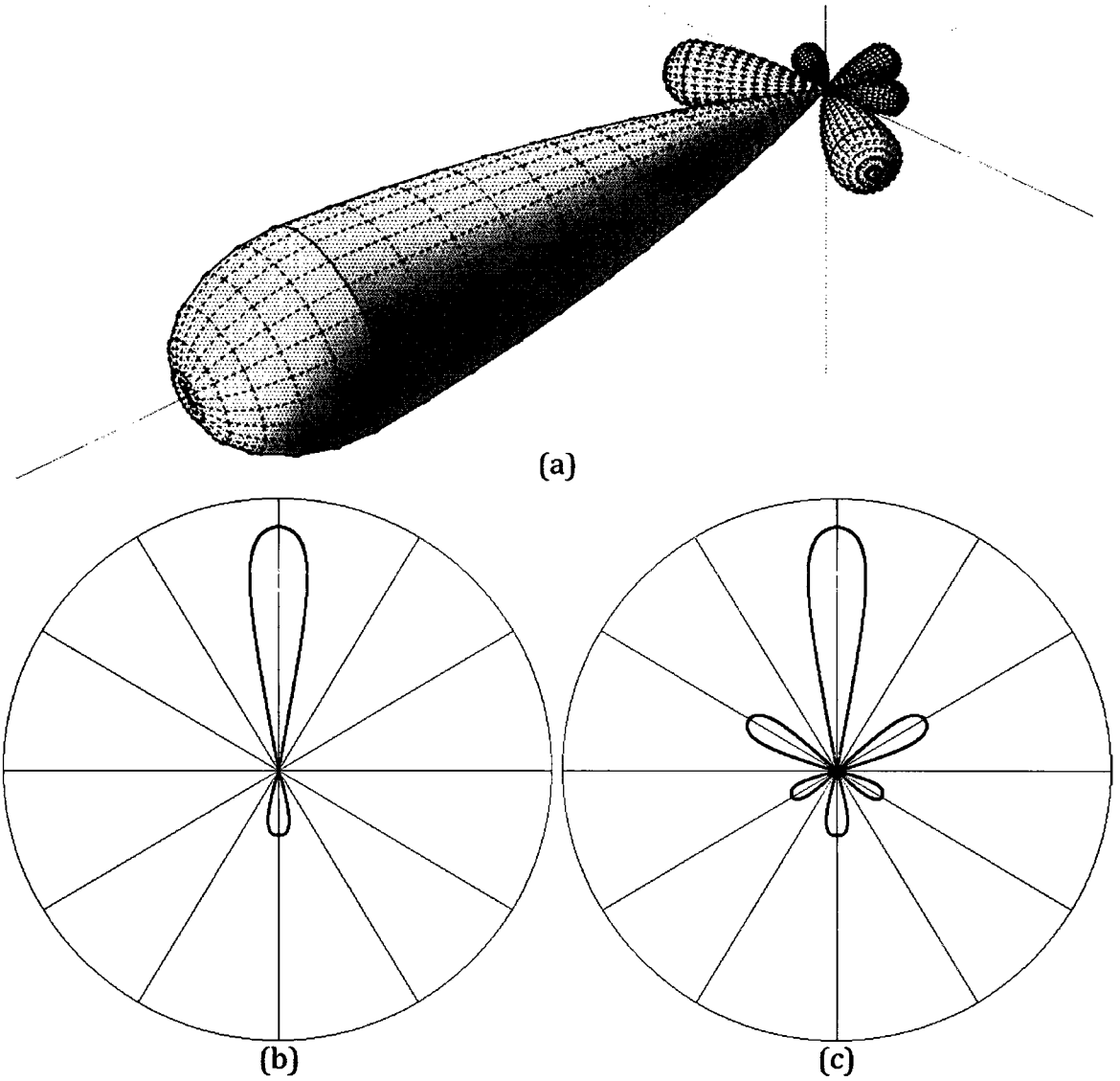

Figure 2-2. Radiation pattern of a directional antenna: (a) 3D polar plot, (b) E-Plane polar plot, (c) H-Plane polar plot.

Other applications may require antennas with a radiation pattern that is highly directive, such as with directional antennas, which radiate or receive more effectively in various directions than others. An example of a directional antenna is the pencil beam antenna, the radiation pattern of which contains a single large, main lobe and several smaller side lobes. Directional antennas are used in applications such as radar or site to site transmissions. An example of a directional pattern is shown in

Figure 2-2. There are other categories of radiation patterns, but omnidirectional and directional are the two main types.

2.1.10 Half Power Beamwidth

Half Power Beamwidth (HPBW) is a measure of the angular size of a lobe in a directional antenna. Taken in a cut plane containing the maximum of the lobe, it is the angular measure between the two directions that are half the maximum as seen in Figure 2-3.

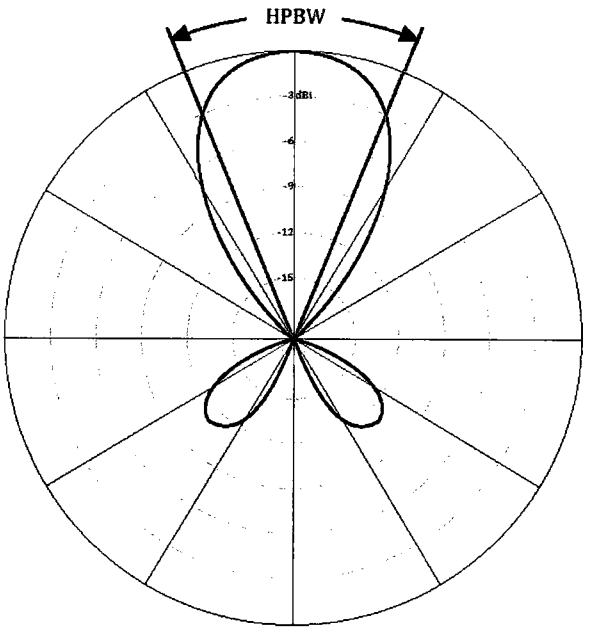

Figure 2-3. An example radiation pattern showing HPBW.

Note that, for some antennas, such as the omnidirectional type, HPBW is not applicable in some planes.

2.1.11 Antenna System Overview

The various terms from section 2.1 are summarized in Table 1. Additionally, for each antenna parameter, such as gain and directivity, there is an analogous partial

parameter. Partial denotes that the effect of polarization mismatch has been taken into account. Also, the overall gain, including impedance mismatches at the antenna input, is called the realized gain.

Table 1. Antenna design parameters. [**15**]

P_{Tx} =	power from the generator.	G_R =	realized gain of the antenna.
P_i =	power incident on the antenna.	G =	gain of the antenna.
P_{in} =	power accepted by the antenna.	D =	directivity of the antenna.
P_r =	power radiated by the antenna.	g_R =	partial realized gain of the antenna.
q_1 =	impedance mismatch between transmission line and generator.	g =	partial gain of the antenna.
		d =	partial directivity of the antenna.
q_2 =	impedance mismatch between transmission line and antenna.	p =	polarization efficiency of the system.
		U =	radiation intensity.
e =	radiation efficiency of the antenna.	U_n =	partial radiation intensity.

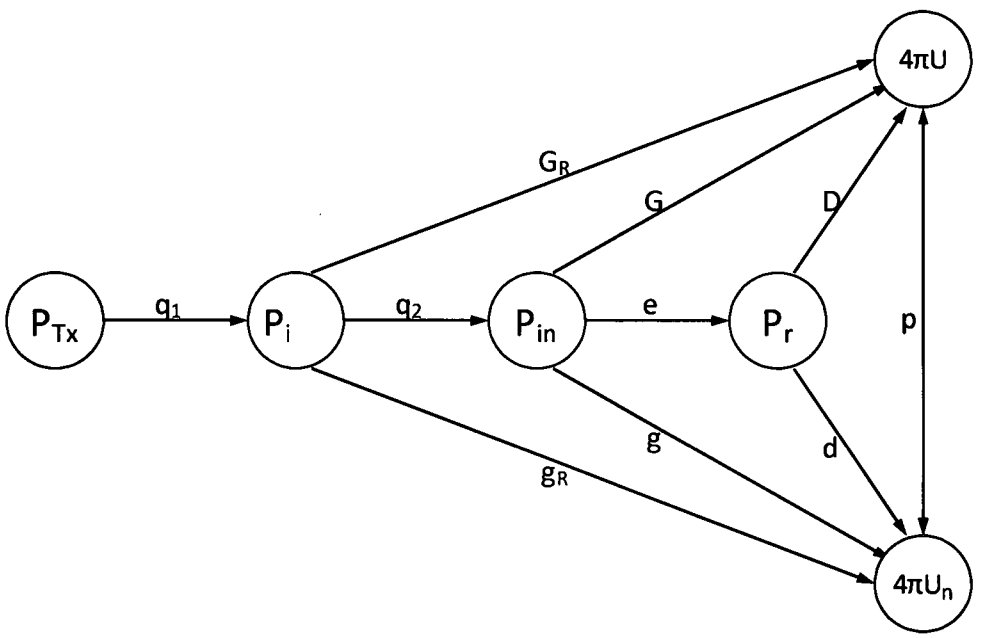

Figure 2-4. Antenna specification flow chart. [**15**]

The terms in Table 1 are represented graphically in Figure 2-4 as the flow of power from the signal generator to the radiated electromagnetic field of the antenna. Although the chart represents a transmitter, the figure for a receiver would appear

similar, with the direction of power flow reversed and appropriate variable name changes, due to reciprocity.

The graph of Figure 2-4 partially represents the Friis transmission equation. The Friis transmission equation gives an overview of an antenna system made of a transmitter and a receiver. It is given by:

$$P_{Rx} = P_{Tx} + q_{Tx1} + q_{Tx2} + G_{Tx} + p + G_{Rx} + q_{Rx1} + q_{Rx2} + P_{pl}, \qquad (2.23)$$

where each variable is in dB or dBm, P_{Rx} is the power at the receiving load, and P_{pl} represents the free space path loss and is given by:

$$P_{pl} = 20Log_{10}\left(\frac{\lambda}{4\pi r}\right) \text{ dB}, \qquad (2.24)$$

where λ is the free space wavelength and r is the distance between the transmit and receive antennas. The free space path loss represents the reduction in power density due to geometrical expansion of the traveling wave as it expands spherically from the transmitter and the frequency dependency of the receive antenna's effective aperture. The Friis transmission is a convenient method for specifying antenna systems.

2.2 Ultra-Wideband Communications

An UWB system is defined as one in which the -10 dB bandwidth is 500 MHz or greater or the fractional bandwidth is 0.2 or greater [5] [6]. In general, this is much larger than a narrow band system, which is usually on the order of a few MHz. In

addition, given this large frequency space, UWB systems can make use of 'carrier-less' signals unlike narrow band transmissions, as well as other novel methods to transmit information.

2.2.1 UWB Signal Generation

Other than PSD, there is no strict specification as to how the bandwidth in UWB is to be used, leading to the evolution of various signal modulation techniques [**4**]. The various methods can be categorized as Frequency Hopping (FS), Time Hopping (TH), and Direct Sequence (DS). A fourth method is to use multi-channel conventional modulation schemes at high data rates, an example being Orthogonal Frequency Division Multiplexing (OFDM).

Frequency hopping involves the use of multiple carrier frequencies at various times. In FH, a known user code is used to 'spread' the carrier frequency over time slots. For a given time slot, the system transmits at one frequency, then, in a different time slot, switches to a different frequency as determined by the spreading code algorithm. The length of the time slots can vary from system to system, including continuous carrier changes, called chirp signaling. The bandwidth of FH is determined by the frequency range of the carriers used and not the data rate. The main advantage of FH is interference avoidance allowing multiple users in the same spectrum [**17**].

Direct sequence schemes modify the original signal by multiplying it by a much higher rate pseudo-randomly generated sequence of 1 and -1. Since the code sequence is higher in frequency, it has the effect of spreading the original signal over a

wider frequency band and, thus, the rate of the code determines the bandwidth used. The advantages of DS include resistance to interference (narrow band, multi-user, or intentional jamming), as well as multipath issues.

OFDM creates a wideband spectrum by virtue of combining many orthogonal narrowband sub-carriers over a range of frequencies. Data can then be transmitted using various multi-channel coding schemes where each sub-carrier can operate at a lower rate, but the overall effect is a high rate. Similar to FH, OFDM's bandwidth is determined by the frequency range of the sub-carriers. Like other UWB schemes, OFDM is robust to interference, but can give a better spectral efficiency. [**18**]

Time hopping utilizes impulse radios and, thus, is considered a carrier-less technique. Data is transmitted by way of sequences of very short duration pulses, which are compressed in time, but wide in frequency. The spectrum and bandwidth of the system are controlled by the shape and duration of the pulses. Since the signal is carrier-less, TH transmitters are generally lower in complexity and consume less power.

2.2.2 UWB Antenna Considerations

Irrespective of the type of the UWB system being considered, an UWB antenna must function over the large, 3.1 to 10.6 GHz, bandwidth. Generally, the band of operation is taken as the antenna's impedance bandwidth, measured by return loss or VSWR. However, the other antenna parameters, as discussed in section 2.1, must also suffice for the desired application and band of operation. For example, it is typically

preferred that gain (directivity) and polarization have a constant response over the entire band. This goal does not differ from narrow band designs, except that for UWB the difficulty is increased for such a wide range of frequencies.

In addition, for pulse based modulation, such as that in TH schemes, special considerations are necessary. In these instances the antenna acts not only as a radiator, but also as a bandpass filter, shaping the spectrum of the signal, in some cases even acting as a differentiator. This can lead to distortions in the pulse shapes, making reception and detection difficult, and possibly causing failure of the radio if not accounted for. Thus, the transient response and group delay of the antenna become important considerations. The design aspects of UWB antennas are summarized in Table 2. [7], [9]

Table 2. The comparison of design considerations for UWB antennas. [9]

Constituent	MB-OFDM	Pulse Based
Electrical	✓ **wide impedance bandwidth covering all operating sub-bands** ✓ steady radiation patterns ✓ constant gain at directions of interest ✓ constant desired polarization ✓ high radiation efficiency ✓ constant desired polarization ✓ high radiation efficiency	✓ **wide impedance bandwidth covering the bandwidth where majority of the source pulse energy falls in** ✓ constant gain at desired directions ✓ **linear phase response** ✓ constant desired polarization ✓ high radiation efficiency
Mechanical	✓ small size / low profile/embeddable /easy-integrated for portable devices ✓ compact but robust especially for fixed devices ✓ low cost	

2.3 CMOS Integrated Circuits

There are several different types of integration, typically differentiated by the semiconductor used. For Radio Frequency (RF) analog circuits conventional choices are Silicon Bipolar (Si-bipolar) and Gallium Arsenide (GaAs), which generally have very good high frequency performance. Even so and more recently, CMOS has become a popular option for RF circuits, its performance in some cases matching or exceeding that of the traditionally 'faster' processes due to aggressive downscaling [**19**].

The development of CMOS integration processes has been mostly driven by the digital electronics field [**20**]. As such, CMOS has become a widespread and highly developed integration process, although mainly focused on digital applications. Yet, as the high frequency performance of CMOS has increased, foundries have made analog design libraries available. CMOS analog development can be attractive due to the low cost, ease of manufacture, and compatibility with digital CMOS. The latter is an exciting advantage, opening possibilities for mixed analog/digital ICs.

2.3.1 CMOS Structure

The profile of a CMOS IC is shown in Figure 2-5 and is made up of 3 general layers, the substrate, the oxide, and the passivation. Within each general layer, various other structures are created using lithographic techniques.

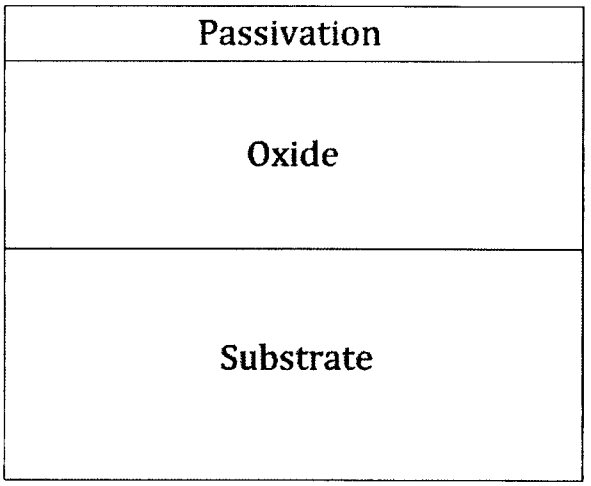

Figure 2-5. General profile of CMOS microchip.

CMOS devices are created in a planar fashion, starting with the substrate and depositing each subsequent layer, using lithography, up to the passivation. This method requires many steps, including adding and removing numerous intermediate layers. Active devices are found in the substrate, near the oxide boundary. The various metal layers, for creating traces and other conducting structures, are contained within the oxide layer. The passivation is a final layer added to provide protection from corrosion and physical damage.

The substrate of a silicon integration process is simply modeled as a resistance in parallel with a capacitance to ground. This represents the lossy coupling of signals to the substrate, which has a low resistivity. Using lumped elements to represent the various electrical parameters, one model for an inductor is shown in Figure 2-6. Being a lumped element model of a continuous effect, more accuracy can be achieved by repeating the circuit, although one may be sufficient for narrow bands.

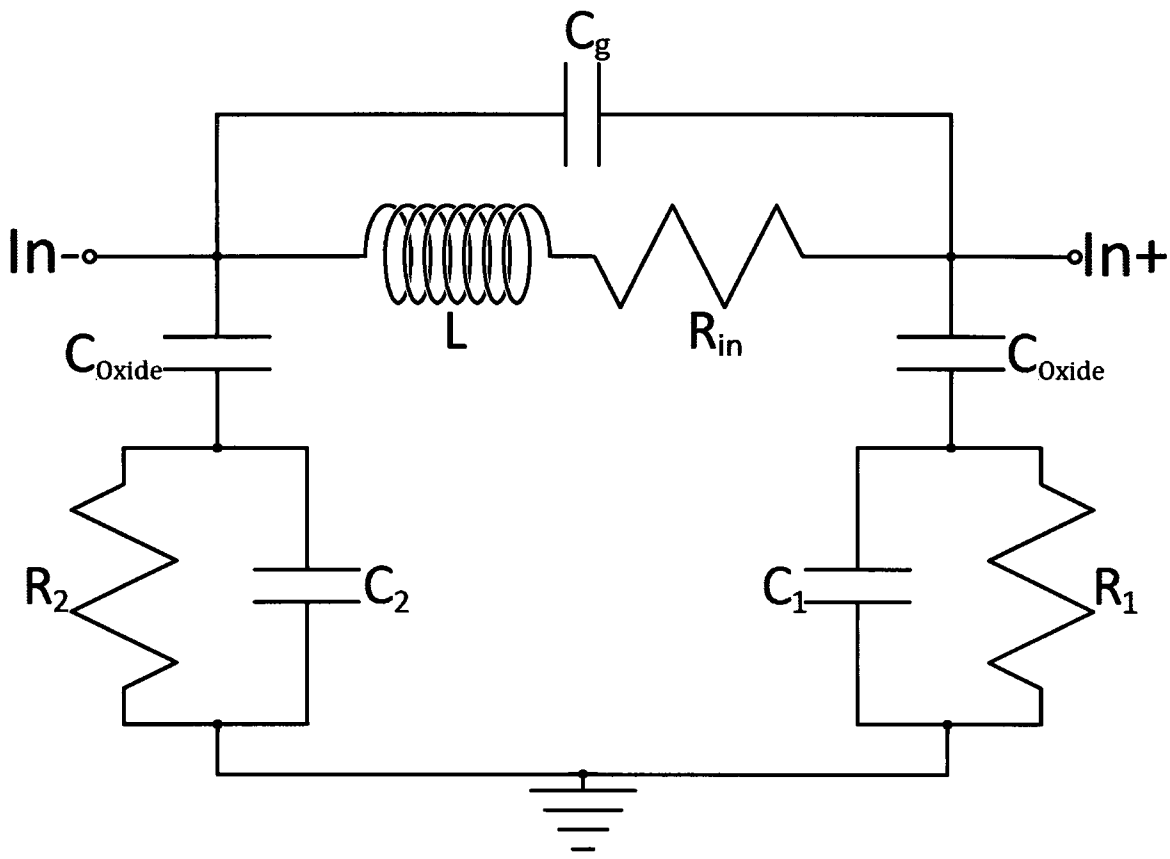

Figure 2-6. Lumped component circuit model of an inductive device integrated in a CMOS process.

2.3.2 CMOS Integrated Antennas

From the perspective of an integrated antenna, the main interest falls on the physical and electrical properties of the 3 general layers shown in Figure 2-5. To remain cost effective, it is necessary to fabricate the antenna using the materials found in mainstream CMOS processes [**13**]. It is the physical structure and properties of these materials that present the first limitations and determine overarching restrictions on the development and performance of an integrated antenna.

Being a planar technology, CMOS is most suited to the use of planar structures. To remain in the paradigm of mainstream CMOS development, the type of antenna used must also be planar. Additionally, the overall size of the antenna must be small, on the order of millimeters, as large ICs are difficult to produce and experience low yields, thus increasing cost. This means, for frequencies in the 3.1 to 10.6 GHz range, electrically small, non-resonant antennas must be used.

Mainstream CMOS processes use a silicon substrate with a resistivity in the range of 10 – 20 Ωcm. The lossy substrate negatively impacts the antenna's ability to radiate power efficiently. In this respect it is prudent to isolate the antenna from the substrate as much as possible, both in distance and by using shielding. Thus it is common to realize the antenna in the top metal layer and use bottom metal layers to form grounded shields. Top metal layers also tend to have the lowest resistivity, thus reducing ohmic losses in the metal. The fabrication process may also allow other methods to increase substrate resistivity, normally used for increasing electrical isolation and reducing substrate noise.

Perhaps the most difficult concern to address is that of structural interferers, although with careful design the effects can be minimized [**21**]. Conducting structures near the antenna can affect its performance, most notably the impedance and gain. This is at odds with the desire to integrate an antenna with a radio in as small an area as possible, which would require placing circuitry near the antenna. In addition to circuit metallization, CMOS processes require dummy metal structures to fill empty areas in order to keep the various planes of the layers level. Although it has

been shown in some instances that dummy fill has a minimal effect on antenna gain and matching for wireless interconnections, this has not been shown to be similar for off-chip communications [**21**].

Chapter 3: Current UWB and On-Chip Antennas

There exist an unlimited number of antennas as any conducting structure can radiate electromagnetic fields. Unfortunately, the performance required of an antenna is application specific and not all radiators will fit the necessary specifications. A good example is that of UWB and integrated antennas.

The main physical constraints in such antennas are due to the realization of an antenna in the CMOS integration process. The antenna must be small, possibly non-resonant depending on the required frequency of operation, and planar. The electrical characteristics of the materials used for integration will also affect the performance of the antenna.

Using an antenna in UWB applications sets the required behavioural properties of the antenna, which in turn influence the shape and structure of the radiator. The design must be matched over a wide frequency range, while also provide a linear phase response and good transient characteristics. The gain of the antenna in the required directions must also be sufficient and as constant as possible over the band.

By combining both UWB and CMOS integration, the possible types of radiators that will operate sufficiently are reduced even more. Various candidates are presented below.

3.1 CMOS On-Chip Antennas

Although the aspiration to integrate antennas on-chip is not new, it is only relatively recent that the techniques necessary to produce such devices in a widespread and cost efficient manner have come into being. As operating frequencies increase (and the corresponding resonant antenna sizes decrease) with the development of mainstream high speed CMOS processes, the ability to fabricate truly monolithic single-chip radios has become a feasible possibility. This is especially highlighted by recent worldwide unlicensed use of the 60 GHz (V) band for high data rate, short range communications. [**22**]

Current CMOS radios are typically small, on the order of millimeters per side, and can be found operating in various frequency bands, including UWB or millimeter wave frequencies. This generally means that integrating antennas on-chip is more feasible at high frequencies, where the wavelength of the frequency of operation is similar to the IC size and antenna radiation efficiency is increased [**23**]. Even so examples of on-chip antennas can be found ranging in operation from a few GHz to more than 60 GHz.

An overview of the simulation of several types of antennas integrated in CMOS is shown in [**22**]. Here it is shown that although the antennas are approximately of resonant size, substrate losses still play a major role in the gain and efficiency of the antennas. Additionally, placement of the antenna, near the corner, the side, or the center of the IC, also plays a role in the radiation characteristics. It was found that Yagi-Uda type antennas have the best directionality, while a rhombic style radiator

has the highest gain, and a loop antenna has almost the same gain, but using much less space.

Two examples of on-chip integrated antennas operating within the UWB spectrum are found in [**24**] and [**25**]. Both antennas are electrically small narrowband loops, the first operating at 5.2 GHz with a size of 1×1 mm^2 and the second operating at 2.5 GHz with a size of 1.62×1.62 mm^2. As expected, the gains of both antennas are very poor due to the antenna size and the lossy substrate (see Section 3.2.5 below and Section 2.3.2 above), but acceptable for short range communications. In both designs the choice of a loop antenna was made to allow use of the area inside the loop for circuitry, making a more compact IC, although in [**24**] the antenna also doubles as an inductor.

3.2 UWB Antennas

The distinguishing mark of UWB antennas is the wide range of frequencies over which they must operate. To accomplish this there are many kinds of UWB antenna designs, which can be categorized as: multiple resonance, traveling wave, frequency independent, self complementary, and electrically small [**8**]. It is not uncommon for an antenna to fall into more than one group. Additionally, having an UWB range of operation does not guarantee that an antenna will meet all required specifications.

3.2.1 Multiple Resonance Antennas

Multiple resonance antennas achieve a wideband response by combining several narrow band radiators into one structure. Since there are effectively an unlimited

number of radiators, multiple resonant antennas can take a multitude of shapes and sizes.

One common type of multiple resonant antennas is the log periodic monopole/ dipole array. Here a series of radiating elements, monopole or dipole antennas, whose sizes and spacings decrease logarithmically, are combined. The log periodic antenna discussed in [**8**] shows a fairly constant gain pattern over the UWB frequency range, although it is not unidirectional. Unfortunately, this antenna does not produce a good impulse response as a large amount of ringing is evident. This is directly attributed to the various resonating elements of the antenna, which introduce frequency dependent non-linear phase responses. Log periodic antennas in general do not produce UWB radiators with a good transient response [**26**].

The elliptical monopole antenna is another UWB radiator that has also been shown to have multiple resonance characteristics [**27**], [**28**]. Despite this, it has also been shown, with optimization of the major and minor axes of the ellipse, the ground plane, and the feed line, that not only is a wideband impedance match possible, but also an excellent transient response [**29**], [**30**]. This is due to the use of smooth transitions, such as those seen in traveling wave structures (see below). A novel example of such a monopole, with good UWB performance, is shown in [**31**]. Another particular feature of interest of this antenna is its relatively compact size, measuring 30.5×38.1 mm^2, which is small for a printed circuit.

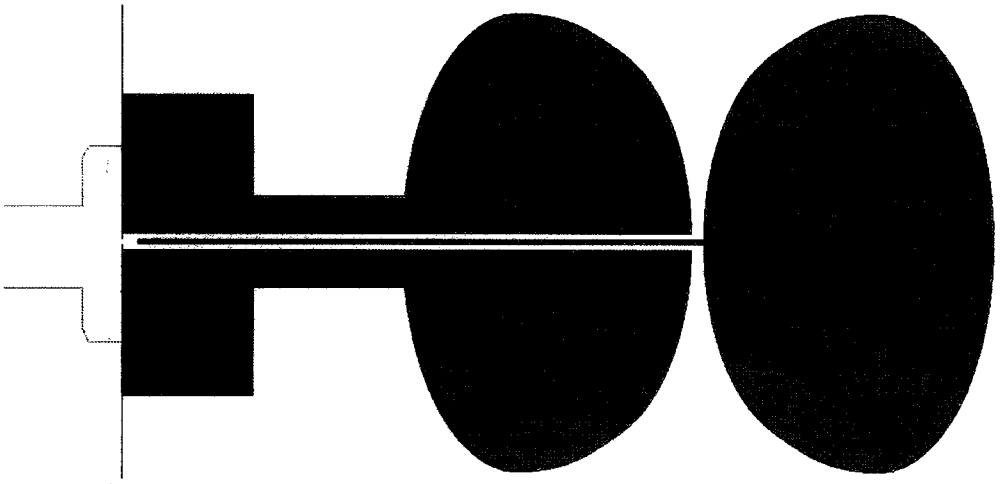

Figure 3-1. The compact uniplanar monopole antenna of [**31**].

3.2.2 Traveling Wave Antennas

A Traveling Wave (TW) structure can be thought of as the counterpart to a resonant antenna. Resonances are standing wave patterns caused by reflections from discontinuities in the structure of an antenna. By smoothing discontinuities, resonances can be avoided. This is accomplished by using continuously tapered transitions, usually from the feed point to the end of the antenna, and tends to create a wide-band response.

The Vivaldi antenna, an example shown in Figure 3-2, is a good illustration of an UWB tapered wave guide antenna [**8**]. An antipodal variation of a Vivaldi antenna is shown in [**32**]. Both Vivaldi antennas display a directional radiation pattern, but have a gain that is constant over the UWB frequency range. Additionally, the transient characteristics show the Vivaldi is suitable for pulsed signal transmission, although its impulse response is not constant with direction.

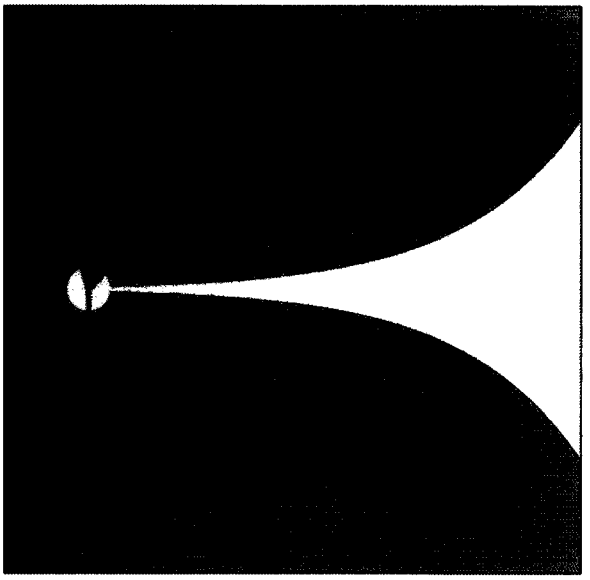

Figure 3-2. An exponential Vivaldi antenna with a Marchand balun feed line on the backside (shown in shadow). This example, taken from [**8**] is 75 × 78 mm².

3.2.3 Frequency Independent Antennas

Frequency Independent (FI) antennas offer the prospect of a radiator that is infinitely wideband. Unfortunately, this also requires that the antenna also be infinite, such as that of the infinite biconical antenna [**14**]. Even so it is possible to design a practical antenna that performs almost constantly over a given band.

The concept of FI antennas is derived from the observation that if a radiating structure is scaled in size, that its characteristics are the same if the input signal's wavelength is also scaled by the same factor. Thus, if an antenna's shape is independent of scaling, it is also independent of frequency. This leads to a class of antennas whose shapes are specified entirely by angles, defined by:

$$r = e^{a(\varphi+\varphi_0)}F(\theta), \qquad (3.1)$$

where r, φ, and θ are the usual spherical coordinates, a is a constant, φ_0 is an angular constant, and $F(\theta)$ is any function of θ. [**33**]

The planar equivalent of the biconical antenna is the bowtie. An aperture coupled bowtie antenna, measuring approximately $36 \times 36\ mm^2$, is shown in [**8**]. This antenna displays an omnidirectional radiation pattern and reasonable gain. It also has excellent transient characteristics with little ringing. Of particular interest is that the impulse response is fairly constant with direction.

A variation of the bowtie antenna, called a rounded diamond dipole antenna is shown in [**34**]. This antenna rotates the two fans of the bowtie so that a diamond shape is created. It is noted that the bandwidth of the frequency response of the rounded diamond is greater than that of a simple bowtie antenna. Another diamond dipole antenna, optimized for a better VSWR over the UWB band, is shown in [**35**].

3.2.4 Self Complementary Antennas

A common subset of FI antennas are Self Complementary (SC) antennas, although being self complementary in itself does not necessarily guarantee constant radiation characteristics with frequency [**36**]. These SC radiators are distinguished by having metal and dielectric patterns that are the same shape and rotationally displaced, two examples shown in Figure 3-3.

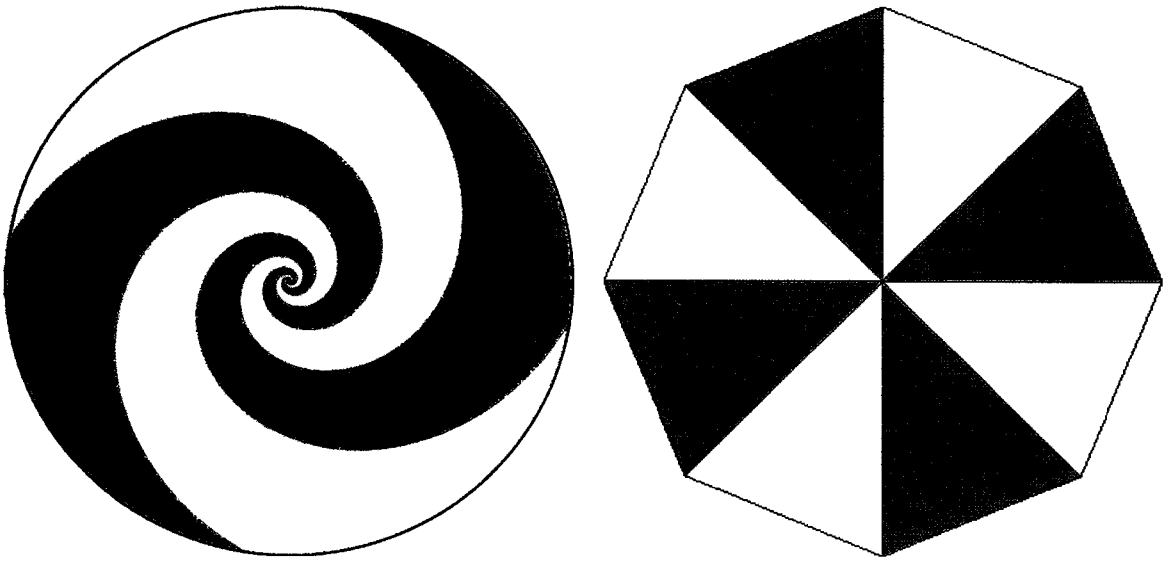

Figure 3-3. Examples of self complementary antennas: (a) logarithmic spiral antenna and (b) octagonal bowtie antenna.

Following Babinet's Principal, the impedance of a self complementary antenna is given by:

$$Z_{metal} = Z_{dielectric} = \frac{\eta}{2}, \tag{3.2}$$

where $\eta = \sqrt{\mu/\epsilon}$ is the intrinsic impedance of the medium ($\approx 120\pi$ for free space). Frequency independence of the impedance is the main feature of SC antennas. This impedance can be varied by changing the ratio of the metallization to the dielectric, although the impedance will not remain independent of frequency.

Another self complementary spiral antenna is the Archimedean spiral. Compared to the continuously increasing line width and spacing of the logarithmic spiral of Figure 3-3a, the Archimedean spiral has a constant line width and spacing. In either case, both antennas radiate circularly polarized fields, requiring pulses of sufficient

length to encompass 360° of the radiated field. Additionally, spiral antennas tend to introduce dispersion into wideband pulses as lower frequencies are radiated further from the center, thus causing a frequency dependant delay. [**8**]

3.2.5 Electrically Small Antennas

An electrically small antenna, sometimes called a non-resonant antenna, is defined as an antenna whose largest absolute dimension, a, is small compared to the wavelength, λ, at the frequency of operation [**15**]. Thus, for an UWB antenna to be electrically small over the entire band, its largest dimension must be much smaller than the wavelength of a 10.6 GHz signal, which, in free space, is $a \ll 28.2$ mm.

An alternate definition for an electrically small antenna is given by:

$$ka < 1, \tag{3.3}$$

where k is the wave number, given by $k = 2\pi/\lambda$ [**37**]. This leads to $a < 4.5$ mm as the boundary for an UWB antenna to be electrically small over the entire band. Although any antenna can be scaled down to become small, various types of antennas lend themselves to this task more easily. Monopoles, dipoles, loops, and their derivatives are common choices [**8**].

Non-resonant antennas display wideband behaviour by performing "equally bad" over the UWB spectrum [**8**]. Since these antennas are electrically small, it is expected that the radiation characteristics, such as maximum achievable gain, will be adversely affected [**38**], [**39**], but in a relatively constant manner and somewhat in-

dependent of frequency. Additionally, small antennas typically present an input impedance that can be highly reactive, making UWB input impedance matching difficult [**40**], [**41**], [**37**].

A miniaturized antenna, approximately 20 × 20 mm^2, is shown in [**42**]. Operating at a frequency of approximately 910 MHz, this antenna uses a split ring resonator to cancel the large inductance of the small loop antenna, making impedance matching much easier. Unfortunately this also has the effect of making the antenna narrow band, but otherwise achieves reasonable gain and efficiency for its small size.

Some examples of small UWB antennas can be found, but are typically not considered electrically small for the entire UWB spectrum [**43**], [**44**], [**45**].

3.3 On-Chip UWB Antennas

Given that, separately, UWB and CMOS integrated antennas present various issues in design and performance, it is not surprising that it is difficult to find an example that combines both technologies. Placing an UWB antenna on-chip requires either a very large IC, which can be cost prohibitive, or using an electrically small antenna, which degrades radiation characteristics. In both cases, substrate losses will affect performance unless some sort of mitigating technique is provided.

Reference [**46**] shows a monolithically integrated dipole antenna with an RF front end, including a Low Noise Amplifier (LNA) and a mixer. This device has an impedance bandwidth over the UWB spectrum and was designed for use with OFDM applications. The antenna achieves a gain of approximately -20 dBi, but transient cha-

racteristics were not measured as that is not required for OFDM applications. Even so, it is assumed that, because this design uses a multiple resonant structure, transient response is most likely poor. In addition, the antenna designed is quite large, measuring 10×0.67 mm^2, although remains less than the wavelengths of the frequencies in the UWB spectrum.

Another UWB fully integrated RF front end is shown in [**47**] with an antenna and an LNA. The antenna is a folded inverted-F with size 4.5×3.5 mm^2, which approaches an electrically small antenna for the UWB spectrum. Additionally, to combat the losses caused by the low resistivity substrate, an Artificial Dielectric Layer (ADL) is placed under the antenna, but above the substrate. The ADL increases the effective permittivity and shields the antenna from the lossy substrate. Use of the ADL was not demonstrated to be overly effective as the antenna gain was approximately -30 dBi over the UWB, but theory predicts an ADL with greater permittivity could improve this. Use of the ADL introduces a tradeoff between antenna performance and chip space as circuitry cannot be placed under an ADL. Transient characteristics were not measured, but due to the resonant features of this antenna it is expected they are poor.

Chapter 4: On-Chip UWB Loop Antenna

When integrating monolithic radiators, the small size of ICs dictates the use of electrically small antennas in the UWB spectrum. This, combined with the losses due to a low resistivity substrate, all but guarantees poor gain and efficiency. Thus, the choice of topology for an on-chip UWB antenna integrated in CMOS is somewhat arbitrary from a performance point of view. Even so, practical applications can still be found for such antennas and therefore the topology used can be determined by other factors, such as minimizing the overall IC area and, thus, reducing cost.

Monopoles, dipoles and loops are common types of antennas that are often found in a below-resonant size. As shown in Section 3.1 and 3.3, it is feasible to integrate these kinds of antennas in a CMOS process and operate them over UWB frequencies. For this thesis a square loop antenna was chosen to be implemented as discussed below.

4.1 Design

The main constraint on the antenna's topology is determined by the IC size. For this design an overall chip size of approximately 1.5×1.5 mm^2 is assumed, sufficient space for a small loop antenna, the UWB LNA designed by Ansari [**48**], and the UWB pulse generator designed by Salehi-Abari [**49**]. By using a loop antenna to circumscribe the circuitry, a large antenna compared to the above given chip size is attained without rendering the entire area unusable to other circuitry. In addition to

maximizing the useful area on-chip, loop antennas are also preferred for applications where the radio is located near obstructions, such as in hand-held or body worn devices. This is due to the fact that loop antennas have a mainly magnetic reactive field, and thus are less susceptible to de-tuning by any local high dielectric constant materials.

The IC was fabricated in a CMOS 0.13 μm process, seen in Figure 4-1. The antenna is fabricated in the top layer metal, shown in blue, and is made of aluminum. Various other metal layers are also shown in other colours, which are mainly seen as power feed lines from the pads located around the right and top of the antenna. These metal layers are found within the oxide layer of the process, while the top metal layer, except for the pads, is covered in the passivation.

Use of the CMOS 0.13 μm process sets the material properties which will physically and electrically constrain the design, shown in Table 3. It is noted that the effective relative permittivity of the structure is a weighted average of the three layers and somewhere between 4 and 11.9. In addition, the fabrication process also allows for a special means for increasing the resistivity of the substrate in selected locations. The technique used to accomplish this is unknown, as is the exact final resistivity. Despite this, any increase in the substrate's resistivity is expected to improve the antenna's performance and is therefore implemented on the substrate beneath the antenna (outlined by the dotted orange line as seen in Figure 4-1).

Table 3. Physical and electrical properties of the CMOS process.

Layer	Resistivity (Ωcm)	Conductivity (S/m)	ε_r	Height (μm)
Substrate	13.5	7.407	11.9	300
Oxide	∞	0	4	16.72
Passivation	∞	0	7.9	4

The antenna was made as large as possible, while allowing for ample spacing of the probe landing/power pads and circuitry, and also remaining electrically small over the UWB spectrum. The outer circumference was set to 1mm per side. The line width was simulated from 10 μm to 250 μm in parametric analysis simulation. The results showed the radiation characteristics had little variation over the widths, but the input impedance did change. The input resistance increased with decreasing width, while the inductive reactance increased at a greater rate. A line width of 100 μm was chosen to reduce the lossy effect of the increased resistance, but still remain small enough to fit the LNA and pulse generator within the antenna's loop.

The final dimensions of the antenna give a mean circumference of 3.8 mm. For an ideal small loop antenna with an equivalent circumference and an effective relative permittivity mentioned in the paragraph above, the resonant frequency would be expected to be between 22.8 GHz and 39.5 GHz. Such an antenna, having $ka < 1$, can be considered an electrically small antenna over the entire UWB spectrum.

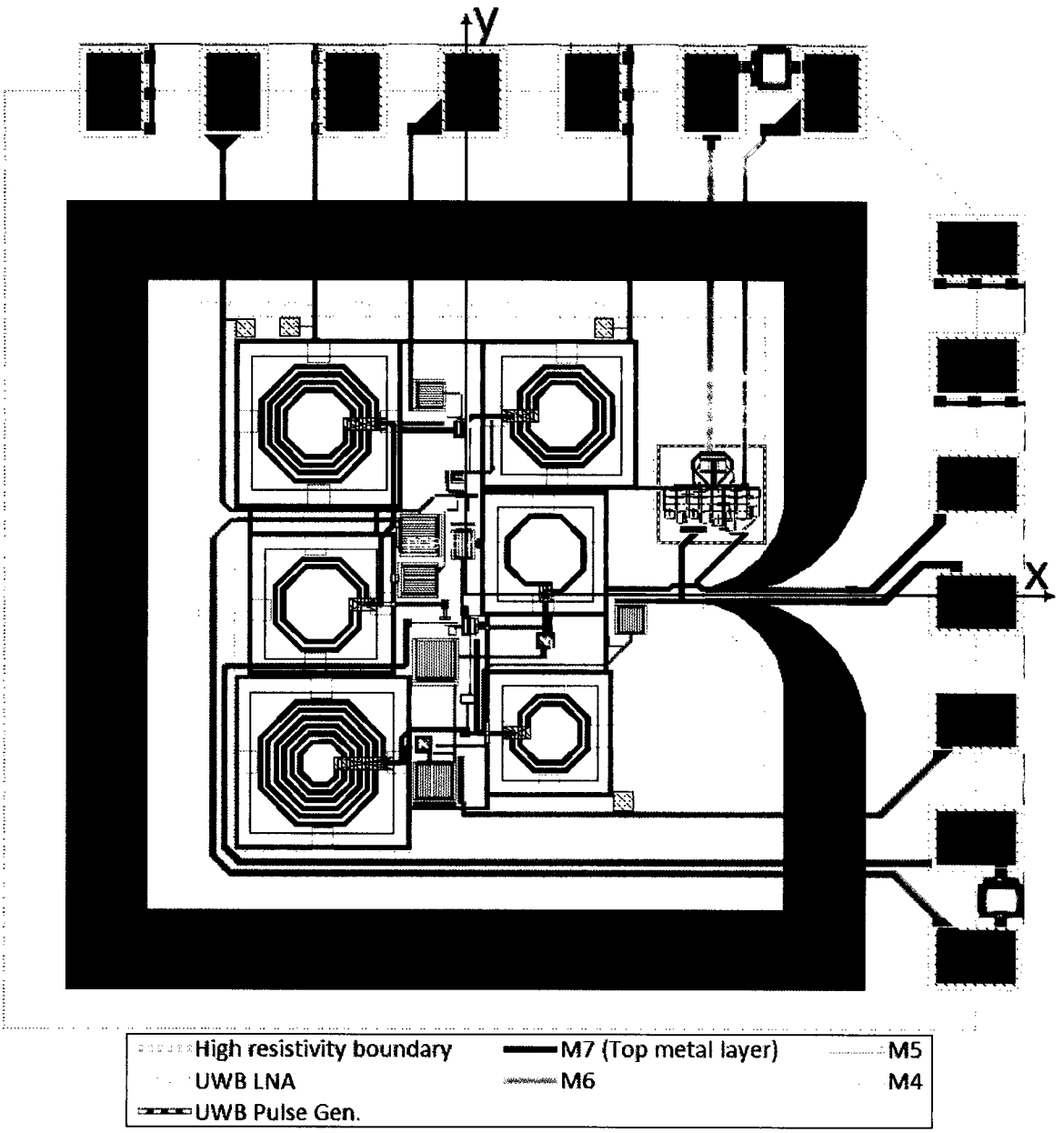

Figure 4-1. Chip layout of a small square loop antenna, UWB LNA, and UWB pulse generator, including probing/power pads. Colours indicate the various metal layers in the CMOS process, as well as highlight some features and circuitry as indicated by the legend.

Inclusion of both an UWB LNA for reception (Rx) (the LNA's capacitors and spiral inductors can be seen in the center of the antenna in Figure 4-1, surrounded by a light blue dashed line) and a pulse generator for transmission (Tx) (seen right of the

LNA and above the antenna's tapered feed lines in Figure 4-1, surrounded by a red dashed line) requires the use of a small network of traces for micro laser cutting, shown in Figure 4-2. Additionally, traces to connect the antenna to probing pads for off-chip measurements are included. Micro laser cutting uses a high powered, highly focused laser to cut through the IC. In doing so, small incisions can be made to separate the Tx, Rx, and antenna for individual testing, while allowing all three to be integrated on the same IC. Although the use of the traces for micro laser cutting may complicate the antenna feed line, it is unavoidable without sacrificing 2 of the three designs as chip space is limited.

Unlike typical designs, the antenna feed lines are directed inward, since the LNA and pulse generator are located within the loop. The feed lines are elliptically tapered along a 90° bend to facilitate a wideband impedance transition from the antenna to the circuitry. Although, at these electrically small sizes, using tapered impedance matching may prove ineffective, it should not hamper performance and may avoid unwanted resonances, similar to that discussed in Section 3.2.2 without adding great complexity.

The LNA and pulse generator are placed within the loop antenna such that the input of the LNA and the output of the pulse generator are as close to the feed lines as possible. Since the LNA is not differential, one side of the antenna's feed lines is grounded, while the other side is connected to the LNA input (noted as gnd. and RF_{in} respectively in Figure 4-2). The pulse generator drives a differential signal (noted as

pulse+ and pulse- in Figure 4-2) and therefore presents no problems connecting to the antenna.

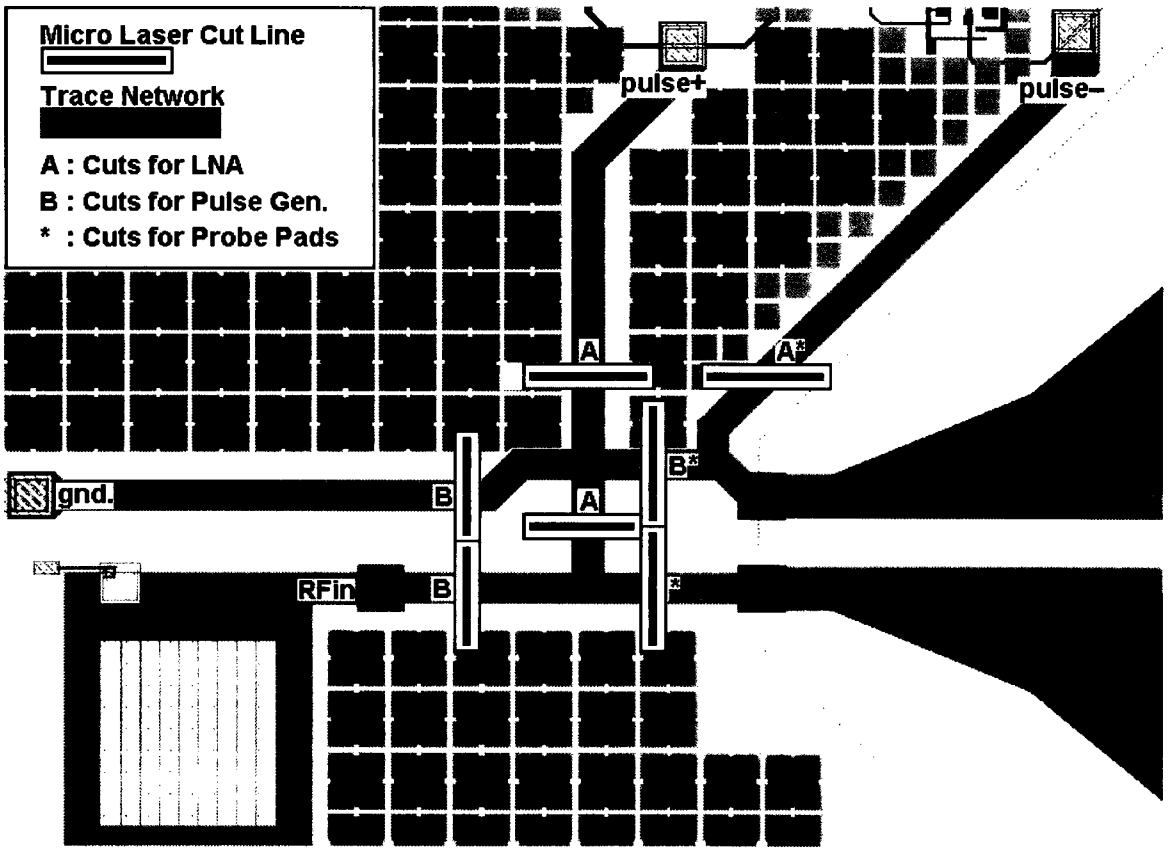

Figure 4-2. Micro laser cuts and input trace network for combining and separating the Tx, Rx, and antenna circuits. The green and orange squares represent dummy fill metal. Note: two cuts are not shown, which are located to the right and remove the lines going to the probing pads for operation of the LNA and pulse generator.

4.2 Simulation

The antenna was laid out and simulated using Ansoft High Frequency Structure Simulator (HFSS). HFSS is a full-wave 3D electromagnetic simulator that can provide "E- and H-fields, currents, S-parameters and near and far radiated field" for any geometry [**50**]. For this project HFSS was used to design, simulate, and numerically

determine the S-parameter, impedance, and radiation characteristics of the loop antenna discussed in Section 4.1.

The simulations were conducted using a 1.5×1.5 mm^2 substrate with the heights and electrical properties presented in Table 3. The antenna structure is implemented on the top metal layer, made of aluminum, and is centered on the substrate with the x-axis in the direction of the feed lines, the y-axis in the direction of the pads, and the z-axis up, out of the passivation (corresponding to the right, up, and out of the page respectively in Figure 4-1). The antenna is differentially driven, across the two feed lines, with a 50 Ω sinusoidal 1 volt source.

3 simulations were performed: a lossless (0 conductivity) substrate with the antenna alone, a lossy substrate with the antenna alone, and a lossy substrate with metal interference structures (pads, etc.). In the lossless simulation the maximum gain and radiation patterns were calculated. In the two lossy simulations the maximum gain, radiation patterns, return loss, input impedance, phase, and group delay were calculated.

4.2.1 Radiation Patterns

The radiation patterns for each of the 3 simulations were created for three frequencies: 3.1 GHz, 7 GHz, and 10.6 GHz. The radiation patterns for the simulations are shown in Figure 4-3 (3D) and Figure 4-4 (2D). It was noted that for the 3 simulations all were similar in shape, having negligible differences. The patterns are omni-

directional in the XY-plane, parallel with the antenna, as is expected for a small radiating loop. It is also noted that the pattern begins to bow inwards along the y-axis,

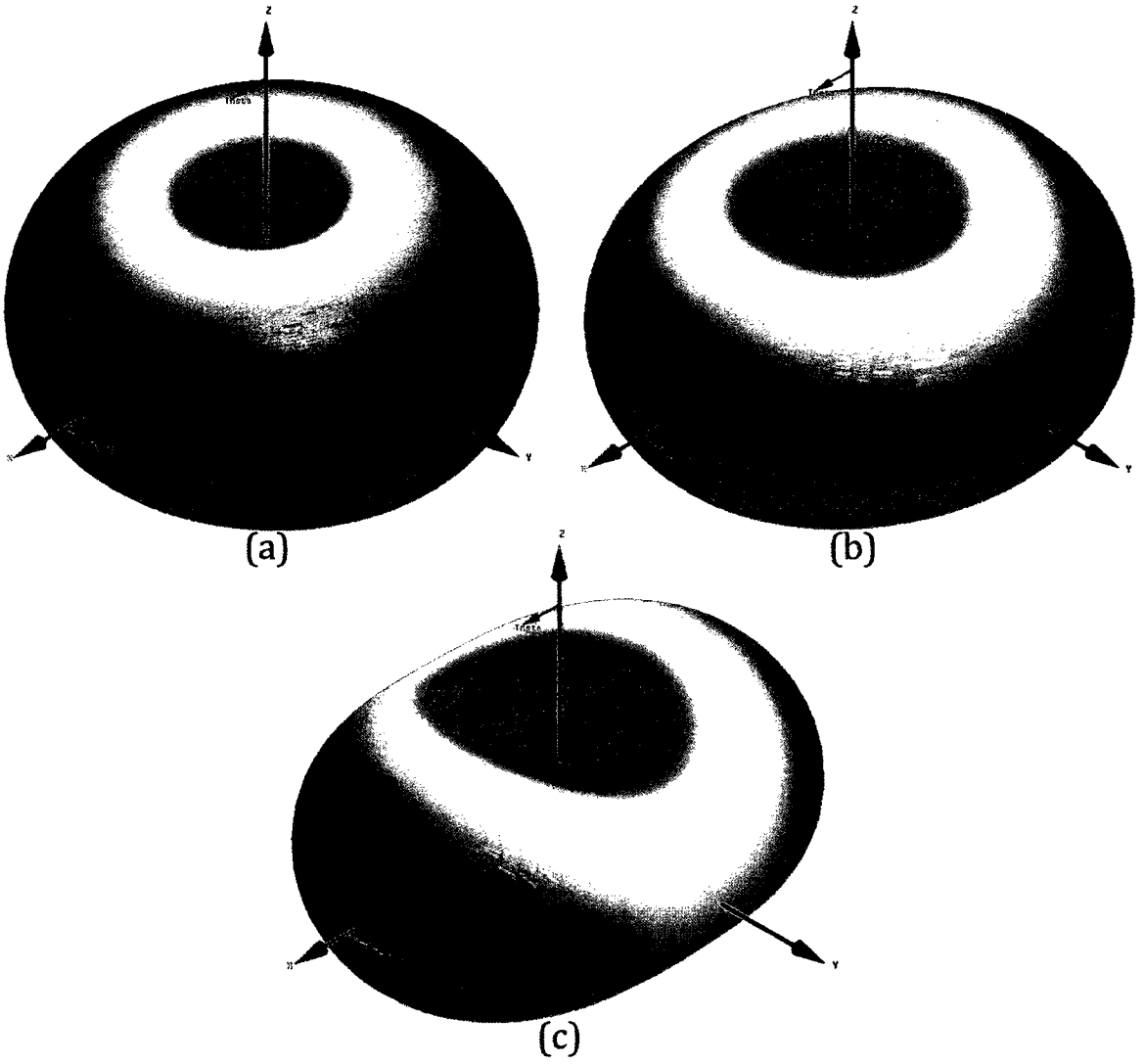

Figure 4-3. 3D radiation patterns at various frequencies: (a) 3.1 GHz, (b) 7 GHz, and (c) 10.6 GHz.

perpendicular of the feed lines on the x-axis, as the frequency increases. This is expected, as, at resonant frequencies, the loop antenna's omnidirectional radiation pattern would change to become perpendicular to the plane of the loop (omnidirectional in the XZ-plane) [**14**].

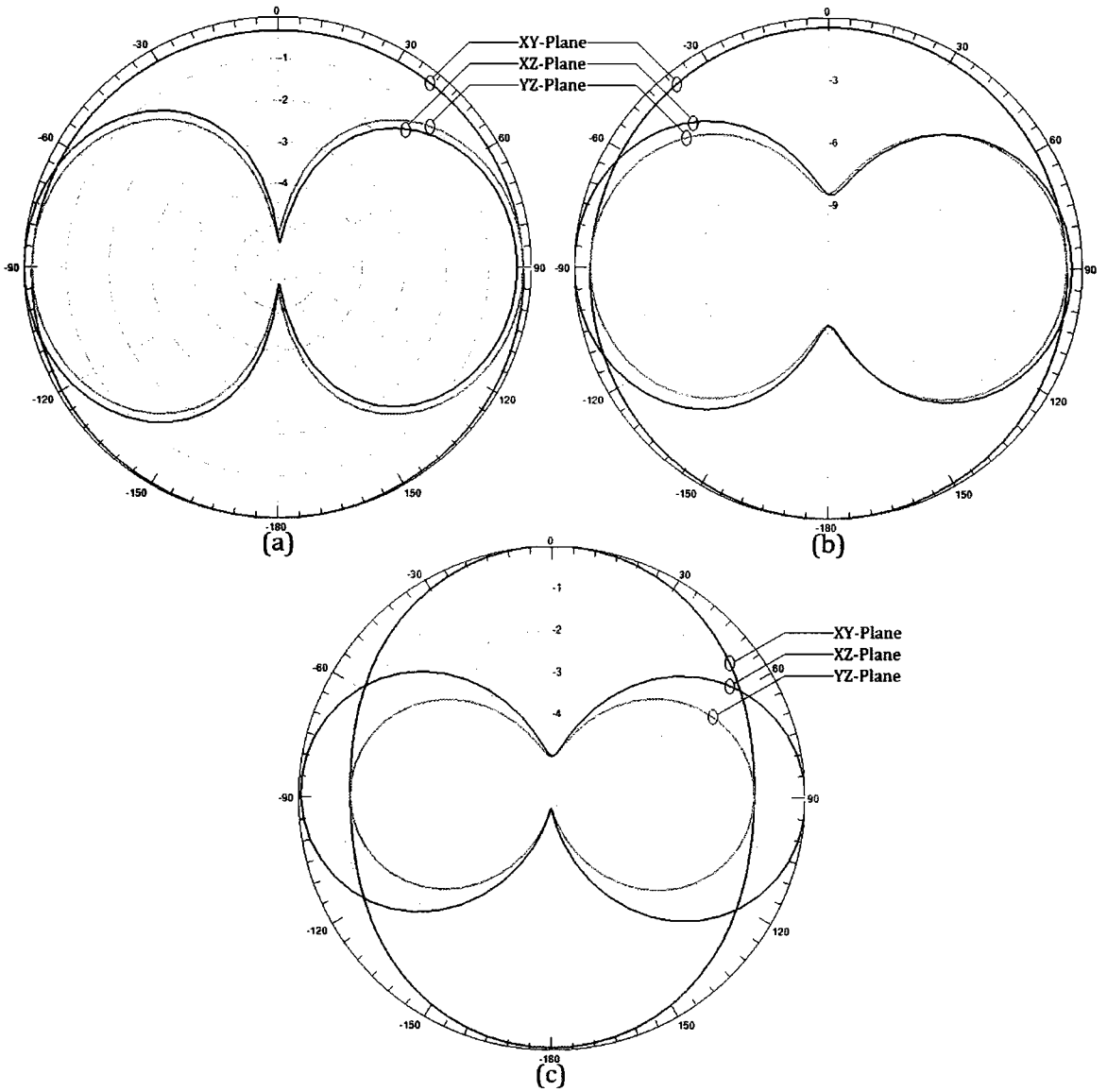

Figure 4-4. Normalized 2D radiation patterns at various frequencies: (a) 3.1 GHz, (b) 7 GHz, and (c) 10.6 GHz.

4.2.2 Maximum Gain

Figure 4-5 shows how the maximum gain is variable as a function of frequency and the substrate resistivity, but is negligibly affected by interfering structures placed around and inside the antenna. As expected, in all cases, the gain of the small loop antenna is very poor and made worse by the lossy substrate, but does improve with frequency as the antenna approaches resonance. In addition, the effect of the lossy

substrate increases with frequency as shown by the increase in the difference between the gains of the lossy and lossless cases. This is as expected as coupling to the substrate, modeled as a resistance in parallel with a capacitance, increases with frequency.

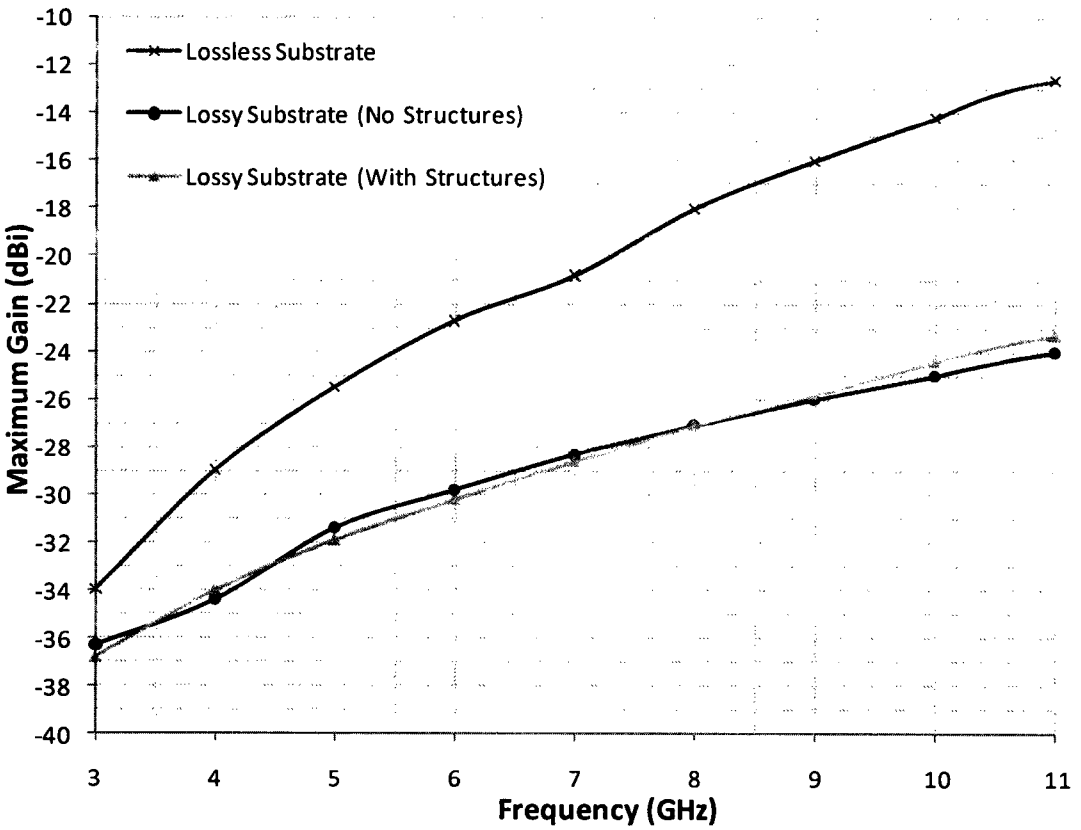

Figure 4-5. Maximum gain of the antenna for each simulation at various frequencies.

4.2.3 Return Loss and Input Impedance

The return loss of the lossy simulations is shown in Figure 4-6. As expected, the match between the antenna and the 50 Ω voltage source is very poor, but only varies by about 0.5 dB over the UWB spectrum. The calculated input impedance of the antenna, modeled as a series resistance and inductance, is shown in Figure 4-7. Similar

to the radiation patterns, the inclusion of interfering structures has a minor effect on the impedance and matching of the antenna.

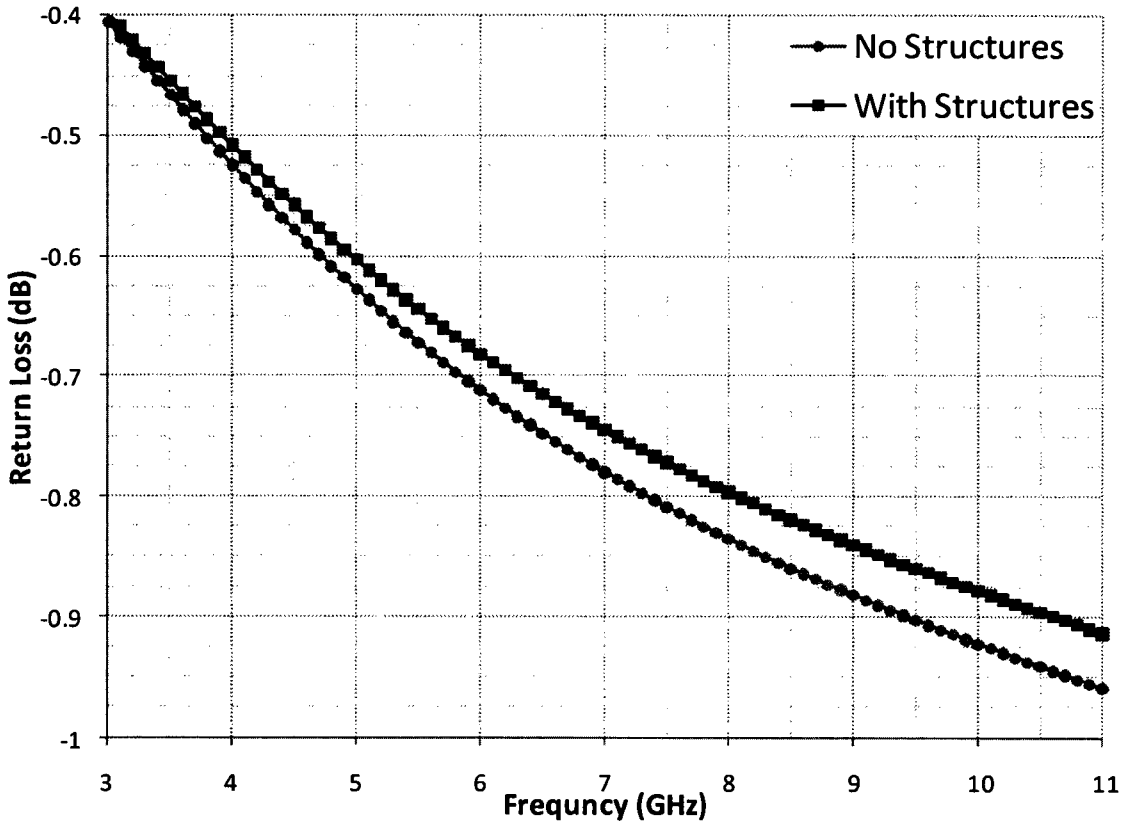

Figure 4-6. Simulated return loss (S_{11}) of the lossy antenna with and without interfering structures.

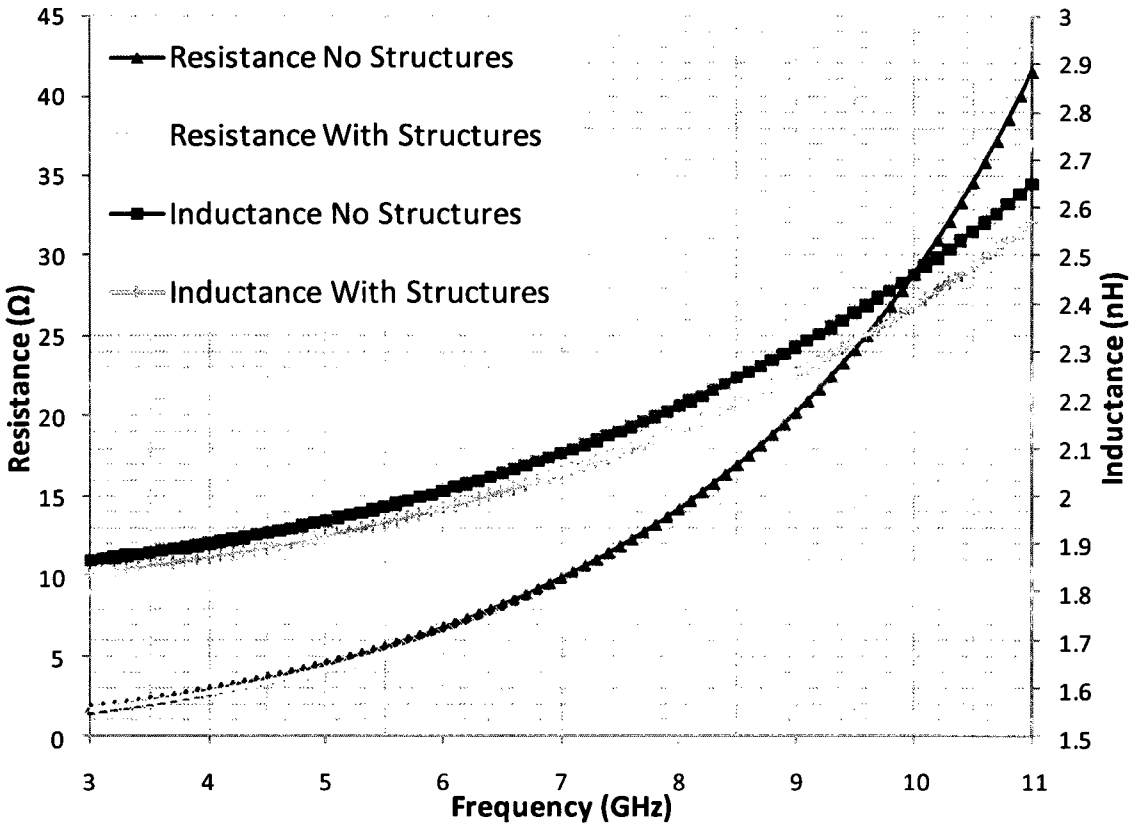

Figure 4-7. Simulated input impedance of the lossy antenna with and without interfering structures.

4.2.4 Phase and Group Delay

Figure 4-8 shows the simulated phase and group delay. Although the phase is not linear, it is close having a linear regression R^2 value of 0.971. This translates to a group delay range from about 15 ps at 10.6 GHz to 52 ps at 3.1 GHz, a variance of approximately 37 ps. Compared to the antennas discussed in Chapter 3:, this is a small value.

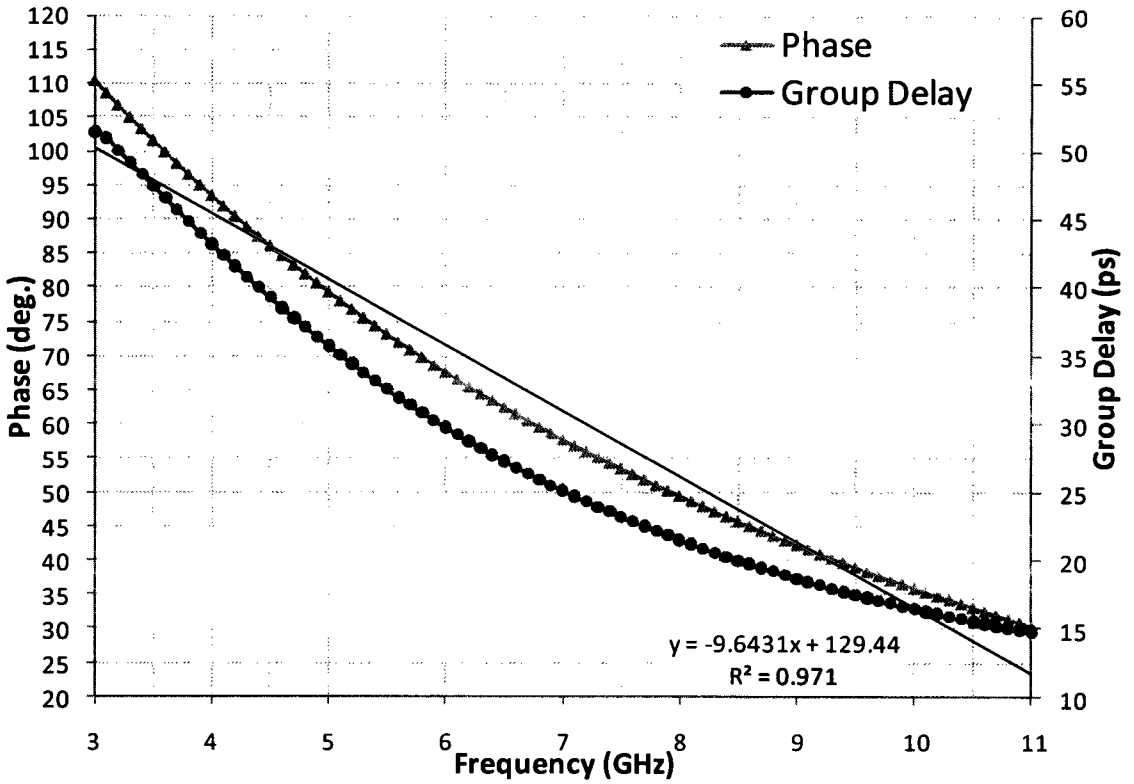

Figure 4-8. Simulated phase response with linear fit and group delay of the lossy antenna.

4.3 Measurement

Measurement of antenna characteristics are generally performed using equipment such as network analyzers, spectrum analyzers, signal generators, and reference antennas with known characteristics. Standard measurements include gain, radiation patterns, impedance, bandwidth, beamwidths, and polarization. These parameters, especially the radiation characteristics, are typically done in an anechoic chamber to remove reflected signals and avoid multi-path issues. A list of the equipment used to perform measurements for this project is shown in Table 4.

Table 4. List of test and measurement equipment used to characterise the antenna.

- Wentworth 907 4" probing station	- HP 83640B frequency synthesizer
- GGB Ind. 40A-GSG-150-P Picoprobe	- HP 8564E spectrum analyzer
- HP 8722ES network analyzer	- HP 54750A digitizing oscilloscope
- BAE H-1498 reference horn antenna	- HP 8131A pulse generator
- 4 pin DC probe	- 1 pin DC probes
- Various lengths SMA coaxial cables	- 1 – 18 GHz spiral antenna
- 109-101C calibration substrate	

Unlike typical antenna measurements, an anechoic chamber was not used during measurements. This was due to the antenna, LNA, and pulse generator being located on-chip, which required the use of a probe station and signal probes to provide power and signaling to the on-chip devices. Unfortunately, a probing station is a heavy and bulky piece of equipment, unable to be practically used in an anechoic chamber. In addition to being outside the anechoic chamber, the probing station itself provides a large source of interference. This is due to its construction being mainly of conducting metals, in particular the large flat metal surface for mounting probes that surrounds the microchip under test. This provides many surfaces near the antenna to reflect signals and create multi-path issues.

It was originally hoped that by integrating the pulse generator and LNA on-chip with the antenna measurement issues involving the probing station could be avoided. By using the monolithic IC, the antenna could have been tested in the anechoic chamber. Unfortunately, both the LNA and pulse generator failed to function in a measureable way and use of the probing station was unavoidable.

4.3.1 BAE H-1498 Broadband Horn Antenna Reference

Before measurements can be conducted, the radiation parameters of the reference antenna are needed. The BAE H-1498 is a linearly polarized broadband double ridged horn antenna. It has a VSWR better than 2 over its operating range of 2 to 18 GHz, matching it to 50 Ω. The gain profile of the antenna versus frequency is shown in Figure 4-9.

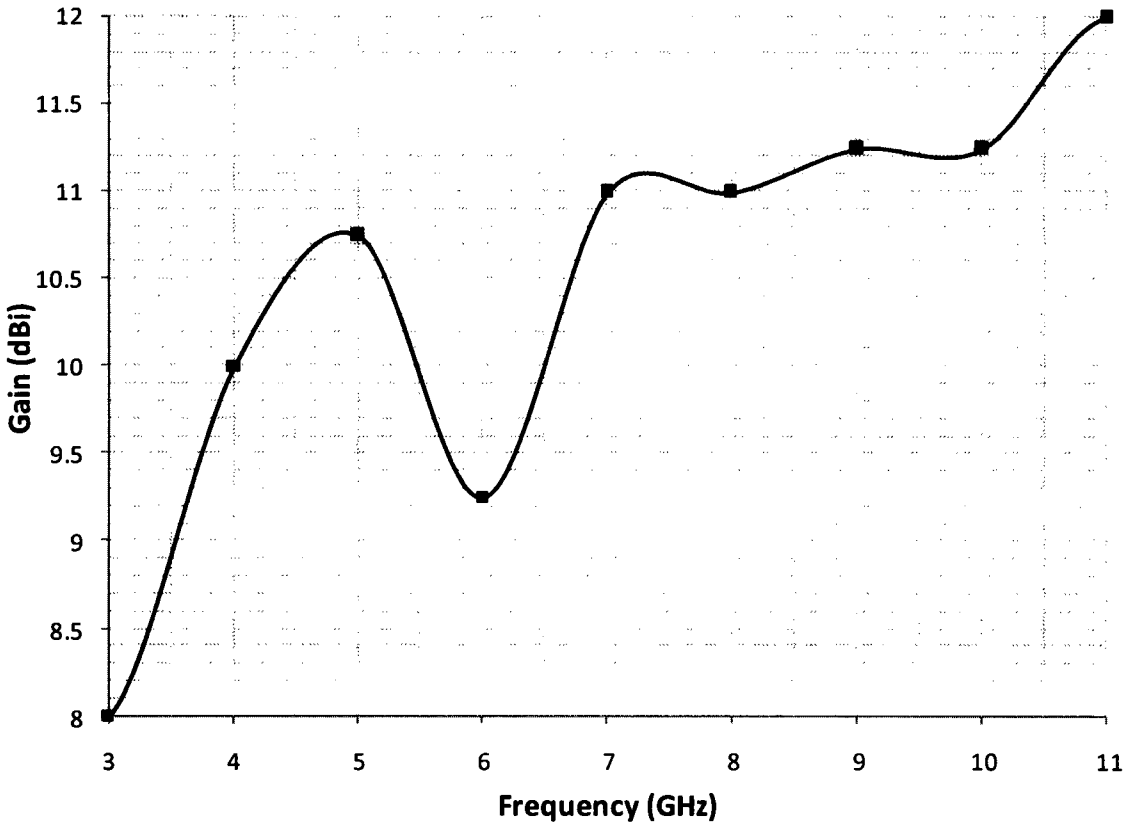

Figure 4-9. Gain profile of the reference horn antenna.

A second wideband spiral antenna was used in conjunction with the spectrum analyzer and frequency synthesizer to confirm that transmission and reception of signals from the horn antenna reference was working.

4.3.2 Transmitter Measurements

To test the IC as a transmitter, the pulse generator and antenna circuit was utilized. The IC was mounted on the probing station and the 2 power pins were supplied via DC probes. A third DC probe was used to connect the on-chip pulse generator's trigger to the HP 8131A pulse generator. A 1 to 1.5 MHz square wave was used to set the pulse repeating frequency of the on-chip pulse generator. The reference horn antenna was connected to the HP 54750A digitizing oscilloscope, which used the external trigger supplied directly from the HP 8131A pulse generator. The transmitted pulse from the on-chip loop antenna could not be detected.

In addition to the above setup, the IC was also mounted on a Printed Circuit Board (PCB) and connected to drive the pulse generator through wire bonds. This was originally done to use the transmitter in the anechoic chamber, but ultimately no pulses could be detected. Despite this, useful experience was garnered involving PCB mounting and wire bonding.

A third testing method was also attempted by connecting a known working pulse generator of the same design from off-chip. This required the use of two RF probes and several DC probes. Unfortunately, the generated pulse was too greatly attenuated by the probes to be usable.

The exact reasoning for the device failure is not known, although troubleshooting seems to indicate a problem with signal propagation between the circuitry and the antenna. Measurements of the DC power draw of the UWB pulse generator indicate

that it is functioning. Increasing the pulse rate increases the DC current draw as expected, signifying pulses are being generated, but no detectable transmitted signal can be found. Although it is still possible that the pulse generator is failing to create a signal, it is more likely that the pulses are attenuated beyond measurability due to impedance mismatches as the pulse generator is designed to differentially drive a 50 Ω load, while the on-chip loop antenna has a mainly (simulated) inductive impedance over the UWB band, seen in Figure 4-7 and Figure 4-16. This highlights one of the key issues with using electrically small antennas; impedance matching can be difficult due to the relative low real and high reactive impedance components.

4.3.3 Receiver Measurements

To test the IC as a receiver, the UWB LNA and antenna circuit was utilized. The IC was mounted on the probing station and the 3 power pins were connected using a 4 pin DC probe. A Ground-Signal-Ground (GSG) RF probe (GGB Ind. 40A-GSG-150-P Picoprobe) was used to connect the RF_{out} on the UWB LNA to the HP 8564E spectrum analyzer. The HP 83640B frequency synthesizer was connected to the reference horn antenna and used to radiate continuous signals at various frequencies at an input power of approximately 12 dBm. The on-chip antenna was illuminated with signals from 3 to 11 GHz, but no signal could be detected on the spectrum analyzer.

Similar to the on-chip pulse generator, troubleshooting the LNA seems to indicate a problem with matching. The LNA, having a maximum return loss of -7.5 dB over the

UWB spectrum, was designed with a 50 Ω input impedance. It is most likely that the signals are attenuated beyond measurability due to impedance mismatching.

4.3.4 Integrated Antenna Measurements

Although unable to use the integrated UWB pulse generator and UWB LNA, and, thus, the anechoic chamber, the antenna was measured directly while mounted on the probing station. Using a GSG probe, the antenna was driven by landing one of the ground pins on one antenna feed line and the signal pin on the other antenna feed line. The second ground pin was landed on a dummy pad. Two setups were used with the antenna driven in this manner: the first involving the frequency synthesizer and the spectrum analyzer, while the second used the network analyzer.

A measurement setup is shown in Figure 4-10. Using this setup, the antenna under test and the horn reference antenna can be connected either to a spectrum analyzer and frequency generator or a 2-port network analyzer. For radiation pattern measurements, the microscope can be removed from the probing station, although the probe and various parts of the probing station will still present obstacles.

4.3.4.1 Antenna Measurements Using Spectrum Analyzer

The first setup connected the antenna, via GSG RF probe, as a receiver to the spectrum analyzer, while the frequency synthesizer was connected to the horn antenna reference for transmitting. The horn antenna was then fixed a distance of 12 cm from the IC in the -X direction in the XY-plane as this is theoretically the direction of

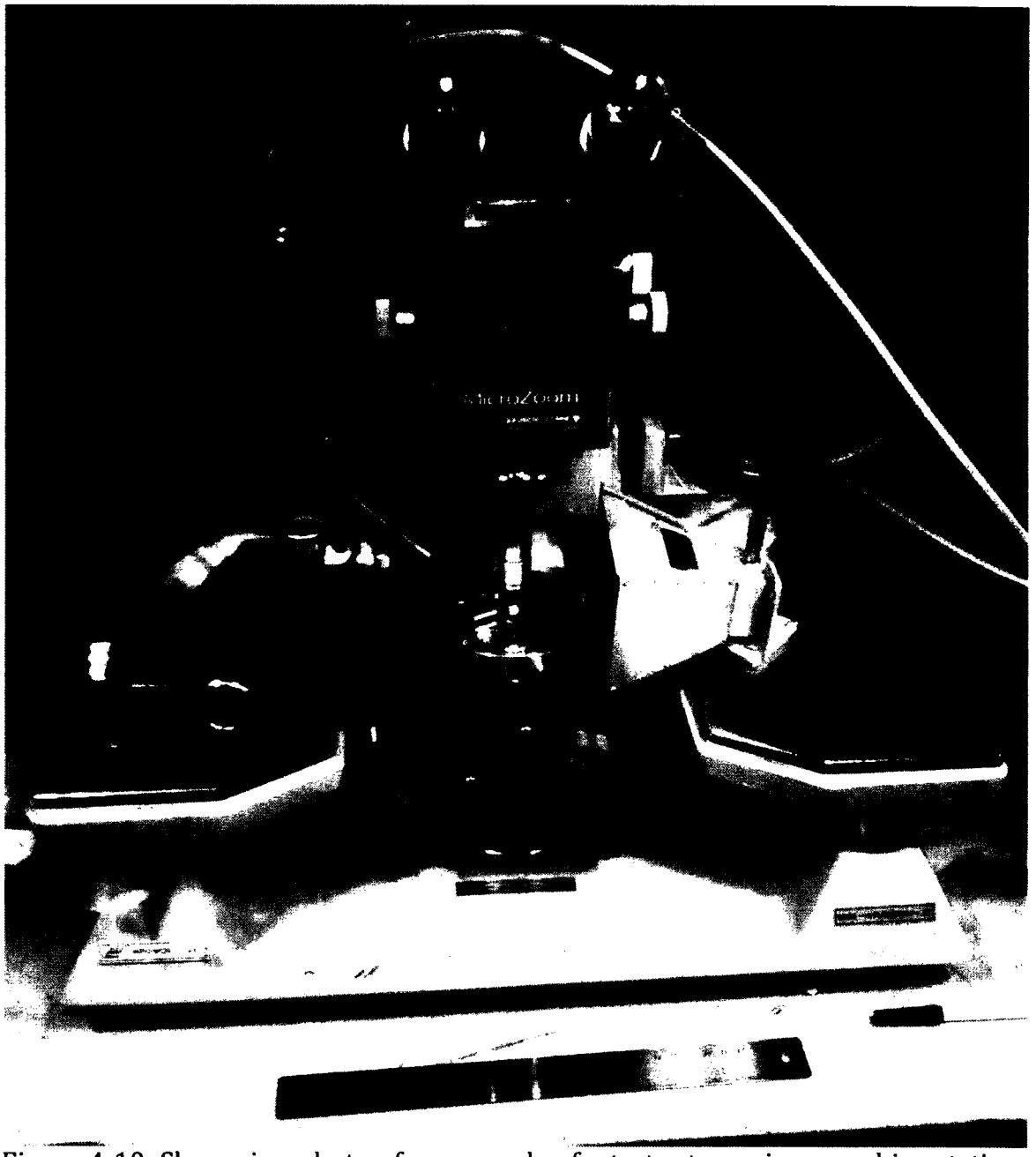

Figure 4-10. Shown is a photo of an example of a test setup using a probing station, an RF probe and mount, and the horn reference antenna. The small square loop antenna is not visible, but located directly under the microscope's objective.

maximum radiation. The radiated signal was then swept over 3 to 11 GHz and the power level from the on-chip loop antenna recorded. The procedure was then repeated with the probe raised above the pads to measure any radiation from the

probe. A final measurement was then made to calibrate the input power at each frequency and account for losses in the cables.

From Figure 4-11 it is seen that the RF probe contributes very little to the transmitted signal. The signal from the probe is 23.2 dB below the signal from the antenna on average and is always less than 11.5 dB. The other feature of note is the variance of the power level of the received signal. This is most likely due to multi-path losses from reflections off the probing station.

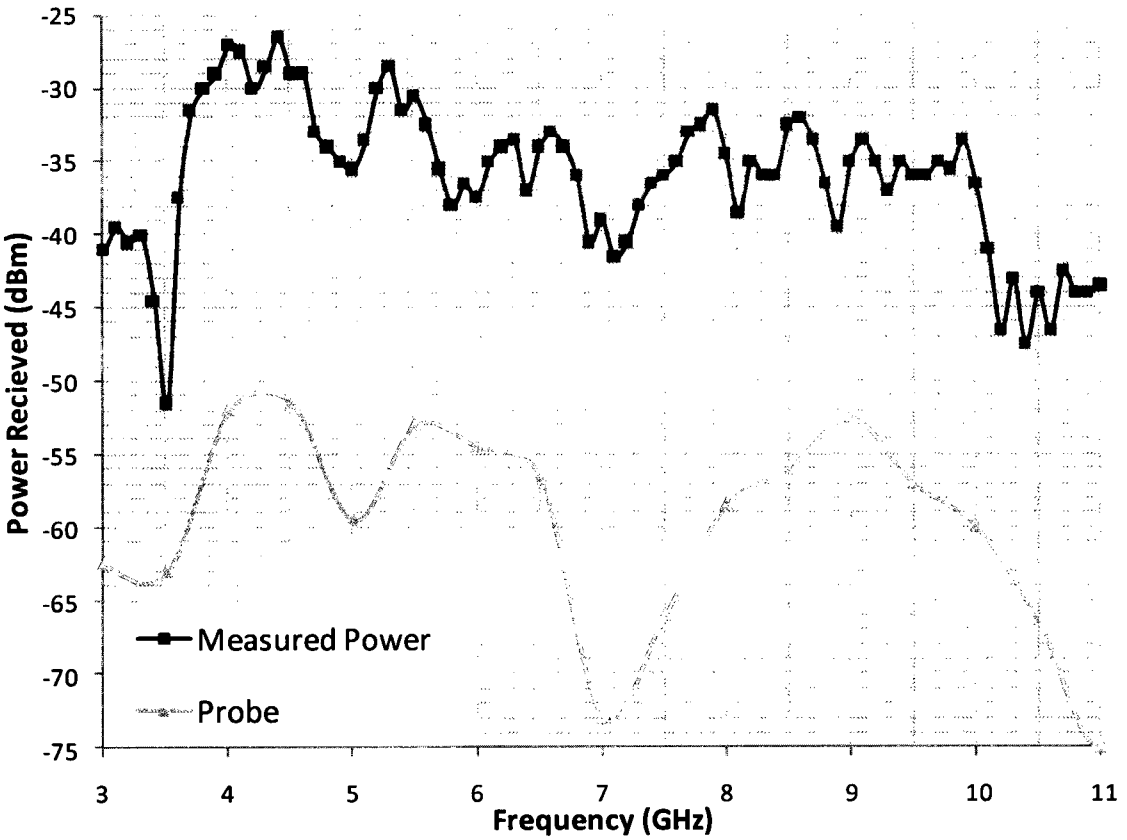

Figure 4-11. Measured transmission path gain of the antenna and a GSG RF probe at a distance of 12 cm.

After correcting for path loss, cable loss, input power, and the reference antenna's gain using the Friis transmission equation, the antenna's gain is seen in Figure 4-12. Polarizatation mismatch was minimized by rotating the horn reference antenna until gain was maximized. The gain is compared to that from the simulation of the antenna with interfering structures. Although the measured levels are variable due to multi-path losses, the general trends of both graphs are similar. A reasonable level of agreement is shown by the red projected fit line, which is only 3dB above the simulated values.

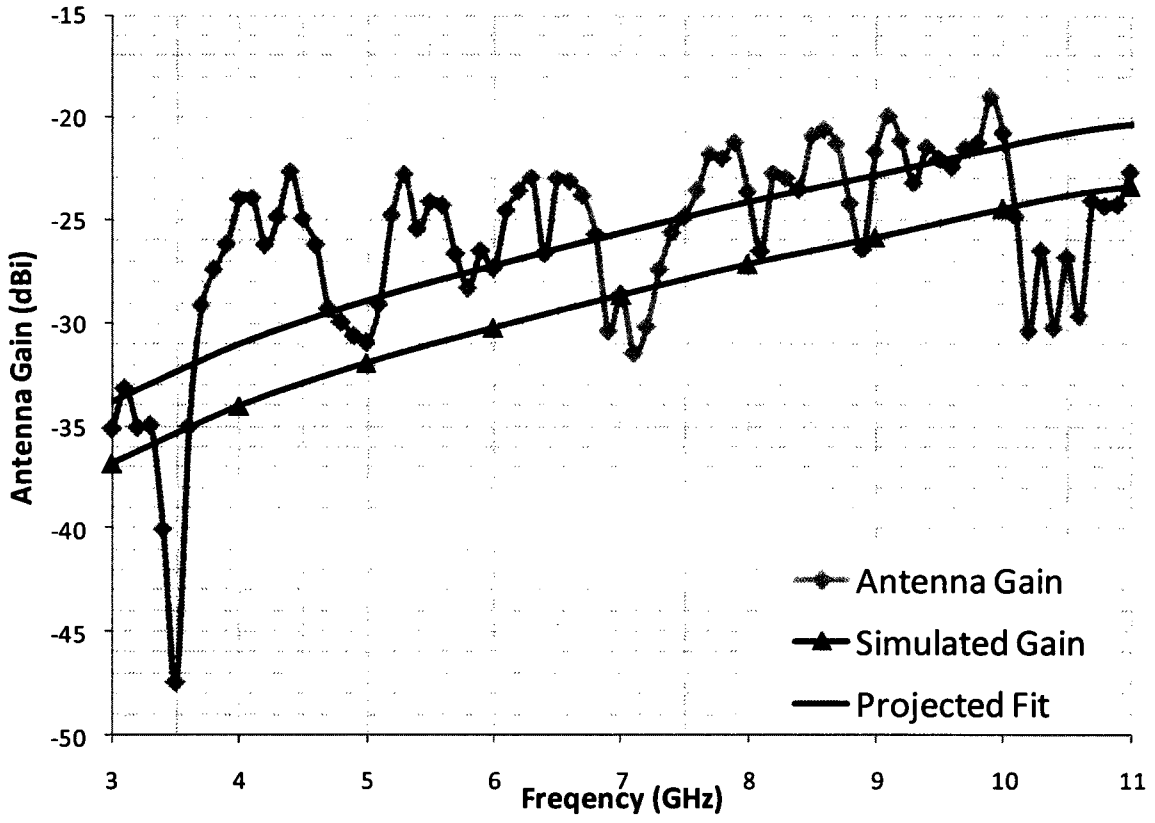

Figure 4-12. Corrected antenna maximum gain measured by spectrum analyzer compared to the simulated gain for a lossy substrate with interfering structures from Figure 4-5.

This setup was then used again to estimate the radiation pattern of the antenna on the IC. To accomplish this the horn antenna was rotated around the IC in the various planes at a distance of 20 cm. Power readings were then taken at various positions and the normalized shape of each pattern sketched in Figure 4-13. Note that the arcs of the measurements are limited depending on the plane as the RF probe (located in the +X direction) and the probing station present obstacles.

The measured normalized radiation patterns are significantly different from the simulated patterns shown in Figure 4-4. Although the XY plane pattern for 3 GHz is somewhat omnidirectional, the XY plane patterns for 7 and 10 GHz are directional. Patterns in the XZ and YZ planes are also very directional, showing multiple lobes. This result is somewhat expected as obstructions (the probe and probing station) around the transmitter greatly affect the direction of the radiation of the antenna due to reflections off the conducting surfaces. This exemplifies the need to use an anechoic chamber for making radiation measurements; otherwise the possibility that unaccounted environmental effects will disrupt an experiment is very likely.

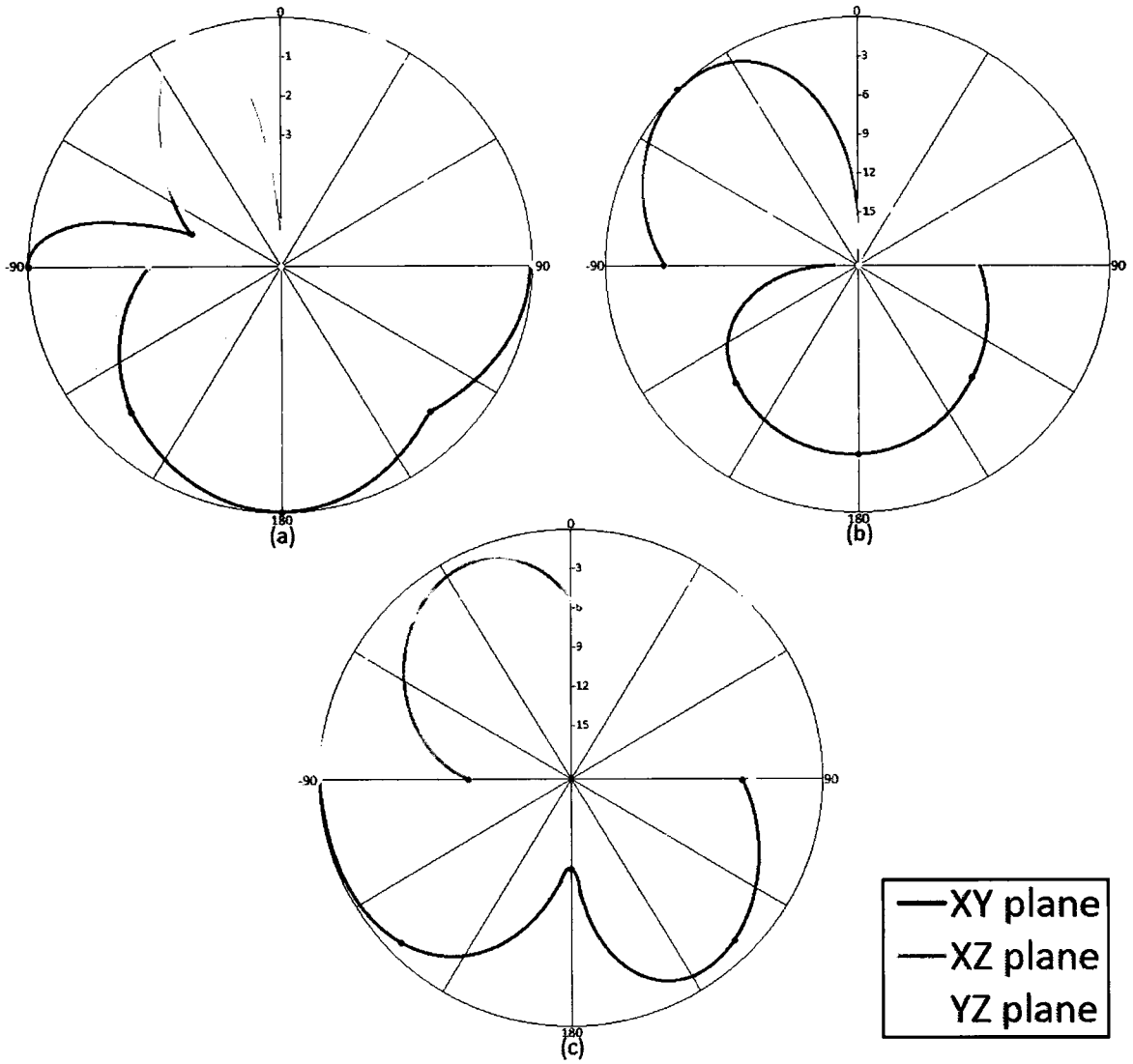

Figure 4-13. Measured and normalized 2D radiation patterns sketches at various frequencies: (a) 3.1 GHz, (b) 7 GHz, and (c) 10.6 GHz.

4.3.4.2 Antenna Measurements Using Network Analyzer

The second setup connected the antenna, via GSG probe, to port 1 of the network analyzer, while port 2 of the network analyzer was connected to the horn antenna reference. The horn antenna was then fixed a distance of 12 cm from the IC in the –X direction similar to the measurement in Section 4.3.4.1. The signal was swept over 3 to 11 GHz at maximum power setting of 5 dBm and the full 2 port S-parameters

measured, shown in Figure 4-14. Before measurements were made with the network analyzer, the system was calibrated using a calibration substrate. This allowed the connecting cables and probes to be de-embedded from the measurements, giving more accurate results, although the horn reference antenna has to be manually de-embedded.

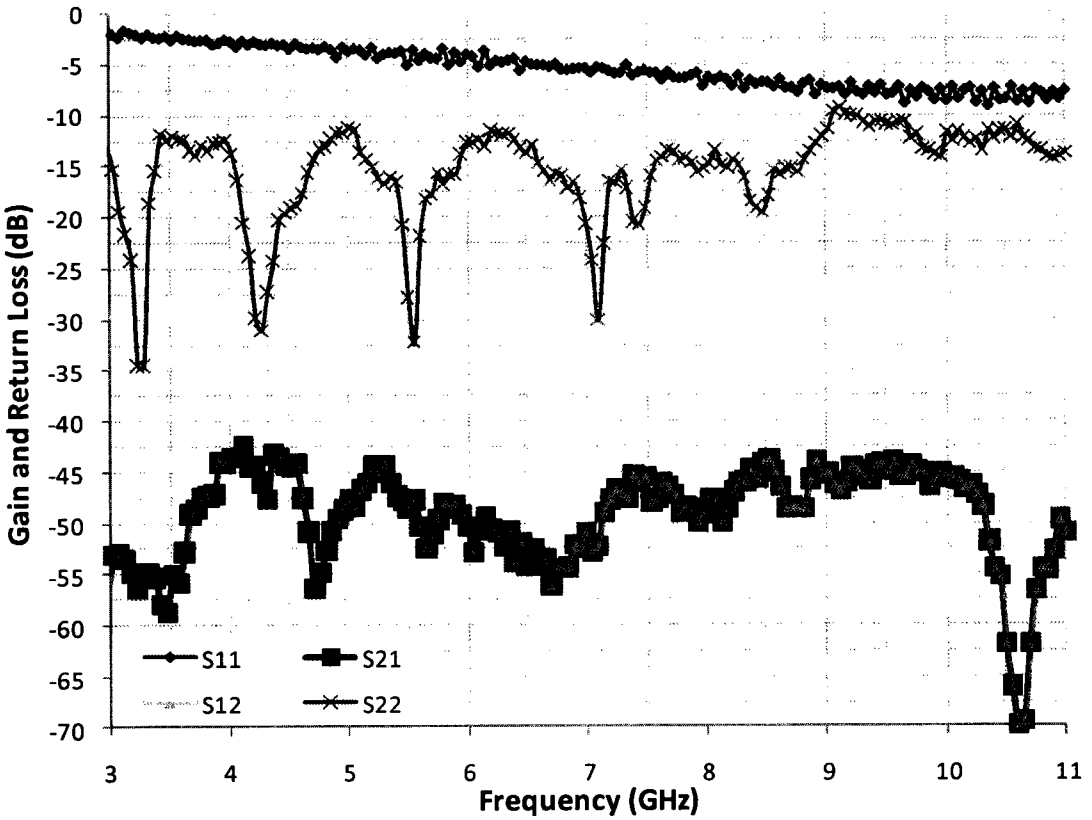

Figure 4-14. Measured S-parameters using network analyzer connected directly to the antenna.

The return loss (S_{11}) can be seen to be poor for an antenna, but significantly better (lower) than that predicted by the simulations, seen in Figure 4-6. Although both graphs show the return loss improving with frequency, the measured value has a range of about 10 dB, where the simulated return loss had less than 1 dB change.

The return loss of port 2, S_{22}, matches the expected behaviour of the horn reference antenna, having a maximum value of approximately -9.4 dB, which is gives a VSWR of 2.

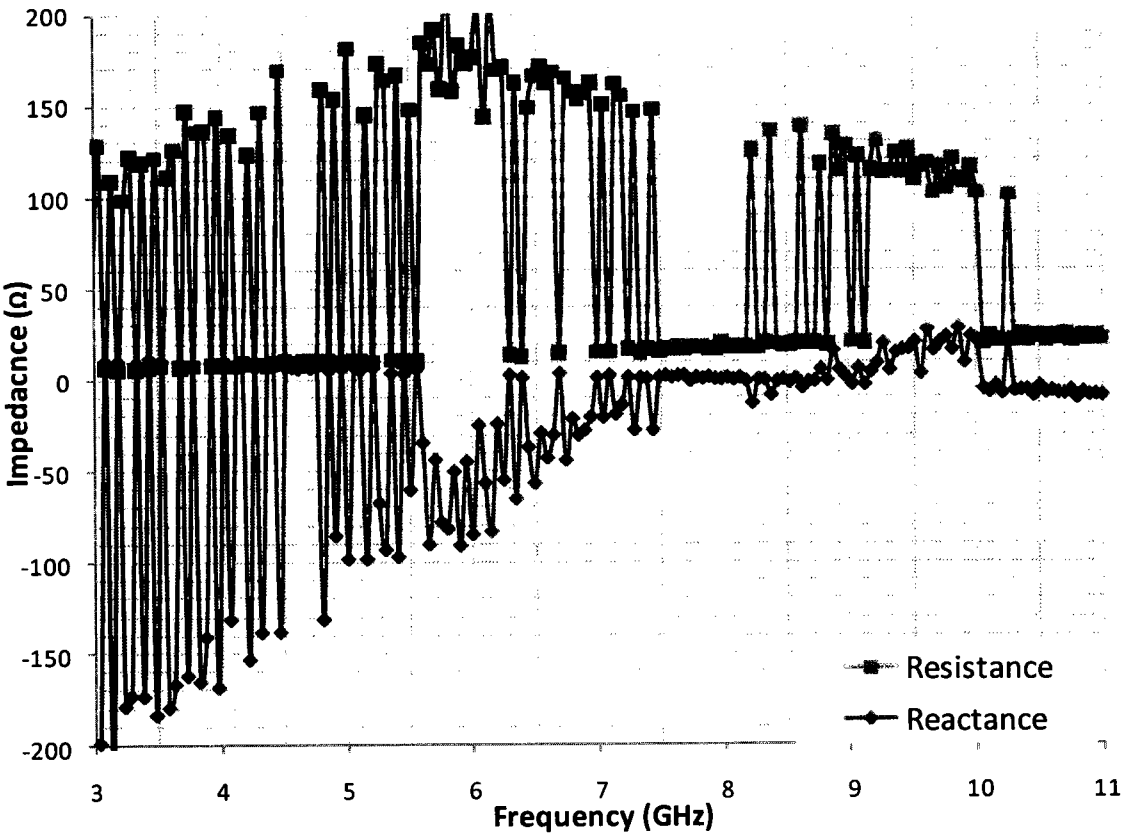

Figure 4-15. Input impedance of the antenna calculated from S_{11}.

Calculated from S_{11}, the input impedance is seen in Figure 4-15. The graph may look somewhat strange, caused by the number of sample points being insufficient to display the high rate of change of the impedances. By qualitative interpolation it can be seen that the impedance is moving through many resonance points over the entire spectrum. This is to some extent more easily seen in the Smith chart of Figure 4-16. Although plot lines are not shown on the Smith chart, what generally happens is the

plot rotates around the circle, slowly spiraling inwards, and crosses the real impedance line many times. This occurs over most of the spectrum, except in the approximate ranges: 5.6 to 6.2 GHz, 7.5 to 8.2 GHz, and 9.2 to 10 GHz, where the plot tends to rotate in place.

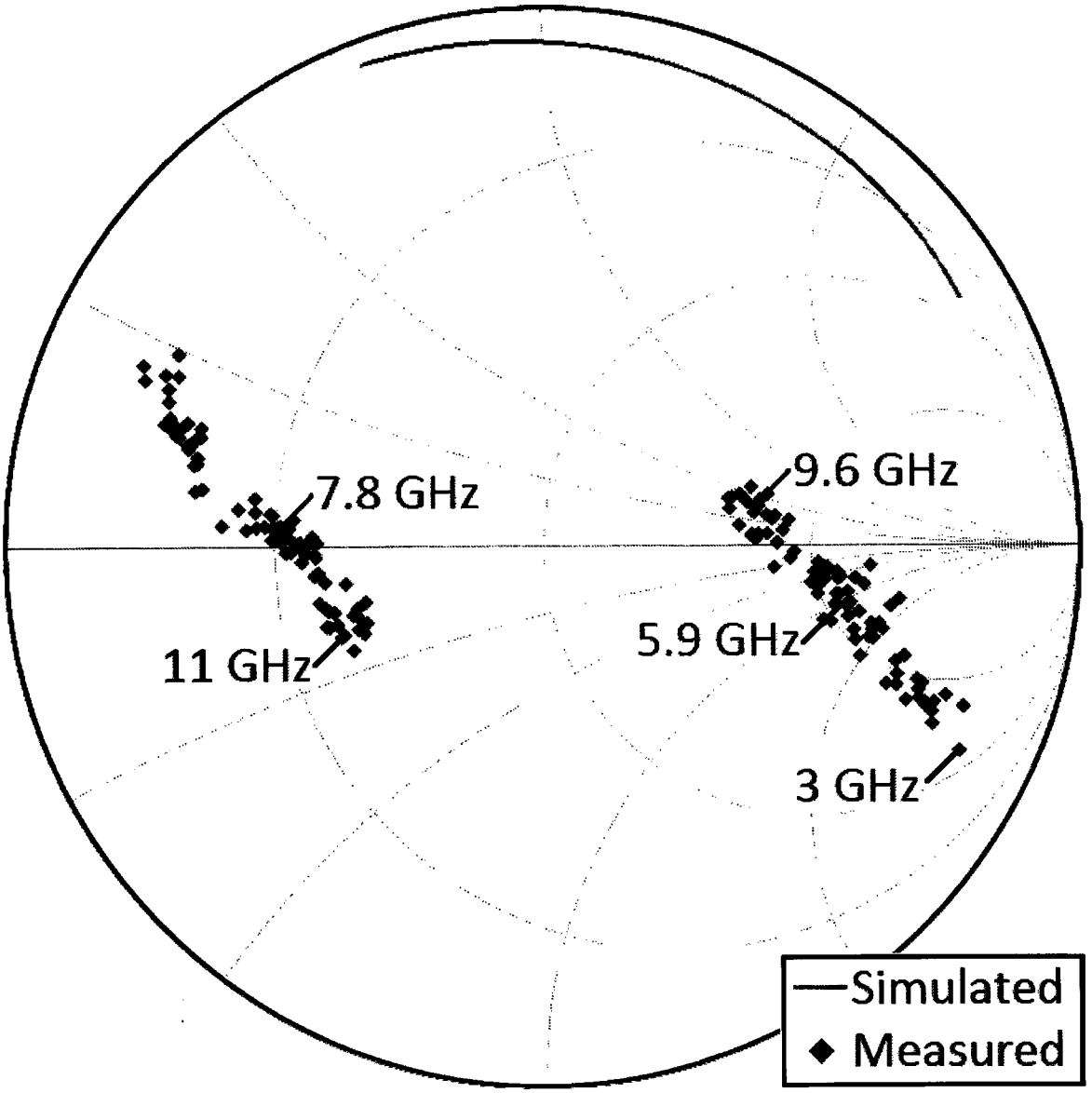

Figure 4-16. Smith chart graph of the simulated and measured S_{11} parameter of the antenna.

The measured/calculated input impedance varies significantly from the theoretical simulation values. Although both rotate around the unit circle with an increase in frequency, as seen in Figure 4-16, the simulated impedance does not cross the real impedance line, staying inductive over the UWB spectrum. This is very different compared to the measured data, which rotates several times around the Smith chart, implying a highly resonant structure. This could in part be due to the probing pads and the lines connecting the pads to the antenna input, which could not be de-embedded with the network analyzer calibration routine.

After correcting for path loss, the reference antenna's gain, and assuming a polarization match, using a modified Friis transmission equation (the calibration of the network analyzer accounted for cable losses and input power), the antenna's gain is seen in Figure 4-17. The gain is compared to that from the simulation of the antenna with interfering structures. Although the measured levels are variable due to multi-path losses, the general trends of both graphs are very similar. There is a high degree of agreement in the measured and simulated antenna gain.

The forward gain, S_{21}, and the reverse gain, S_{12}, from Figure 4-14 demonstrate the reciprocity of the antenna system, both being almost equal. Similar to the measurements in Section 4.3.4.1, the variance in the gain shows multi-path dependencies. Both measurements show dips in the gain at approximately 3.5 GHz, 5 GHz, 7 GHz, and 10.5 GHz.

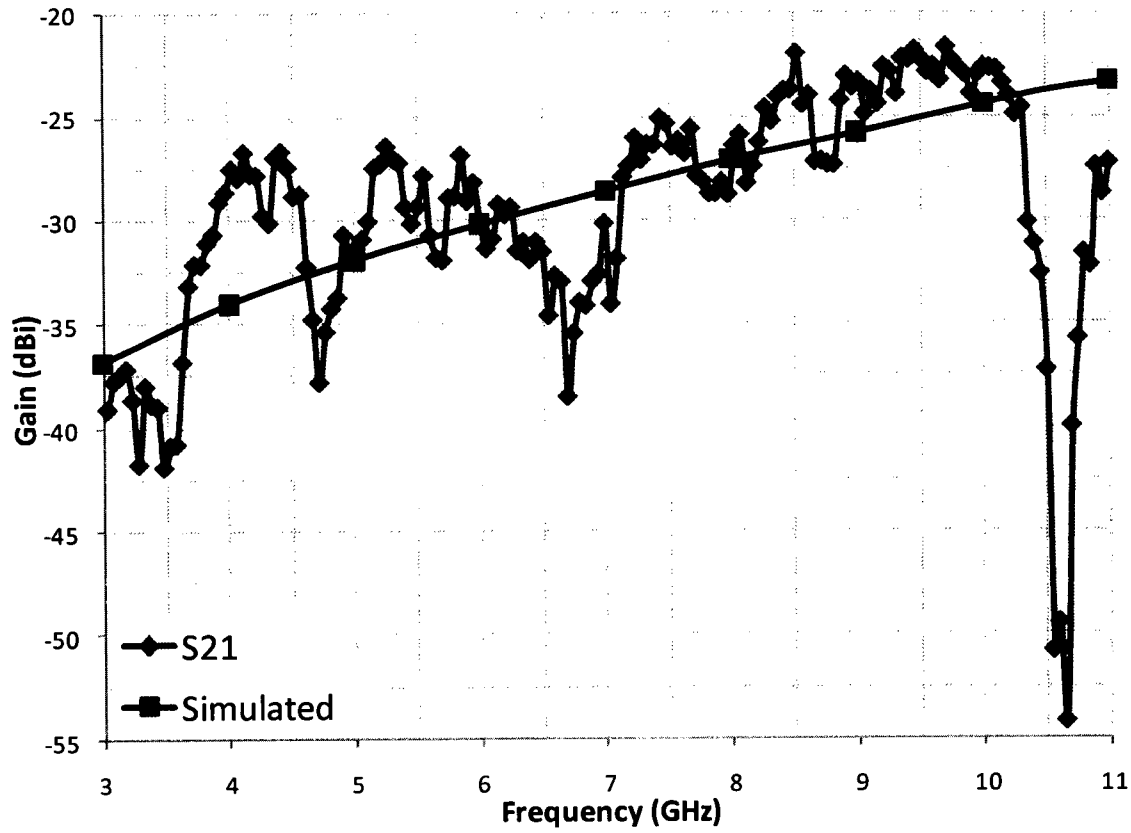

Figure 4-17. Corrected antenna gain measured by network analyzer compared to the simulated gain for a lossy substrate with interfering structures from Figure 4-5.

Measured phase response and group delay are shown in Figure 4-18. The phase is approximately linear with an R^2 value of 0.99 and having a slope giving an average group delay of approximately 1.88 ns. This is a reasonable number considering the path length of 12 cm. The range of the group delay over the entire UWB spectrum is about 10 ns. The large group delay is mainly due to a sharp drop in the phase at about 10.6 GHz, which corresponds to the sharp drop in gain as seen in Figure 4-17 and results in a significant increase in the group delay. Ignoring this point, the range demonstrates a difference of about 4.5 ns, which is more reasonable, but still somewhat large compared to the absolute theoretical minimum of 0.8 ns (0.12 cm path

length). These results are consistent with the other data in indicating that there are significant multi-path effects in the measurements.

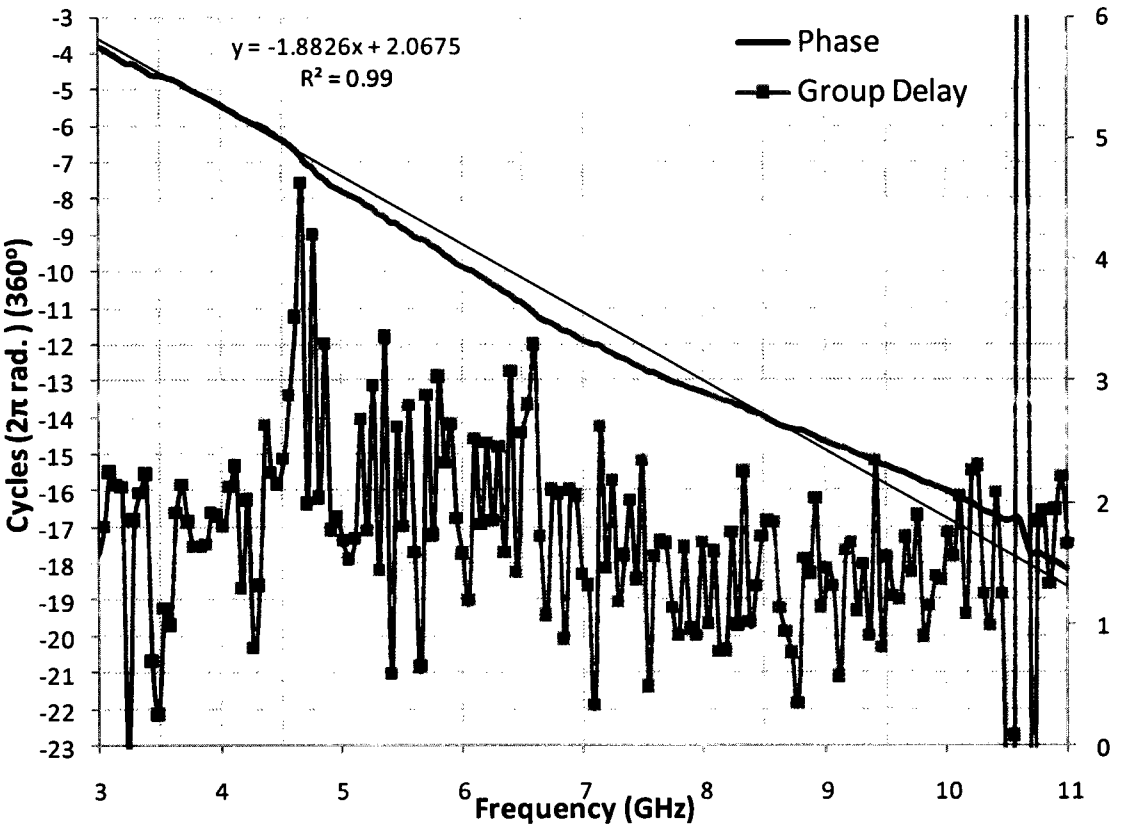

Figure 4-18. Measured phase response and group delay.

Chapter 5: Conclusion

5.1 Conclusion

An on-chip electrically small UWB square loop antenna was integrated onto an IC in a 0.13 μm CMOS process. The measurement results, although not conclusive in demonstrating all the performance parameters, do show that the antenna radiates sufficient power to operate at short distances. The maximum gain varied from approximately -35 to -25 dBi in Figure 4-12 and Figure 4-17, agreeing closely with simulation, and is adequate for wireless devices that need only communicate over ranges less than 1 m. If coupled with a high gain off-chip antenna, such as a horn antenna, this range could possibly be extended to several meters.

The ability to use the antenna as part of an UWB Impulse Radio (UWB-IR) remains uncertain. Since the pulse generator did not function as expected, time domain measurements of the antenna could not be performed. Despite this, the phase response of the antenna from Figure 4-18 does seem to indicate a reasonable level of linearity and thus may provide a constant group delay. Although the transient response of the antenna cannot be confirmed, current data does suggest the antenna still may be viable for UWB-IR.

Although the measured radiation patterns are not omnidirectional, the resulting patterns could possibly be explained by reflections from interfering structures around the antenna. Further evidence that reflections causing multi-path issues exist are seen in the variance of the maximum gain as well as the resonances in the in-

put impedance. Although multi-path problems do not cause the antenna to cease to function, they can render the antenna's radiation characteristics ambiguous. As such, the antenna's radiation patterns cannot be confirmed or negated.

Even though the integrated UWB LNA and pulse generator circuits failed to operate in a measureable way, important information and experience were garnered about the design for test aspects of an on-chip antenna. Perhaps the most notable lesson: the impracticality of driving an on-chip antenna from off-chip. The need to connect the antenna from off-chip severely hampers attempts to characterize its performance. This highlights the necessity to have a functioning signal source on-chip to avoid extraneous components and equipment that may interfere with the antennas operation. Another point of note is the need to better match the input impedance of the antenna with the attached circuitry. Doing so over a wideband for electrically small antennas is difficult and most likely would require co-design of the antenna and circuitry as standard 50 Ω input/output impedances generally will not work.

5.2 Future Work

The main focus of continuing this research includes the creation of a working signal source on-chip. By doing so, several issues and problems would be concurrently solved. The design of the pulse generator, although functional for UWB, was made to drive 50 Ω. It may not be possible to match such an impedance to an electrically small antenna. Thus future work would include co-design of the antenna and pulse generator, ensuring sufficient signal propagation between the two circuits.

As part of re-designing the pulse generator, the transient response of the antenna could also be measured. In addition, with a fully integrated device, the IC could be mounted on a PCB and used in an anechoic chamber. This would hopefully remove any unwanted reflections and multi-path issues.

Re-design of the LNA may also be considered, although it is suggested that this circuit be removed from the IC. Having both the LNA and pulse generator on-chip overly complicates the matching, requiring micro laser cutting to separate the circuits. The LNA also requires probing to measure the received signal, thus not alleviating the original issue. Of course, it may be advantageous to develop both the LNA and pulse generator with the antenna as two separate ICs as operating the LNA and antenna circuit can still provide some data. It may also be prudent to leave the LNA on-chip, although disconnected, to gauge the effect of its presence on the antenna.

As an alternative to using the UWB pulse generator as the signal source, it may be advantageous to use Voltage Controlled Oscillators (VCO). Although VCOs generally are narrow band, there are examples that produce signals across the UWB spectrum. Although a VCO would not allow for transient response characterizations, radiation patterns would be easily measured at the VCOs given frequency of operation.

Although radiation pattern measurements are not practical on a probing station, it may still be worthwhile for determining the input impedance and return loss of the antenna. For such measurements it is recommended that pad and transmission line

de-embedding structures are included in the design. With these structures, more accurate input characteristics of the antenna could be determined.

Once the antenna is fully characterized, integration into a full transmitter and receiver would be the next step. This would also require the co-design of the antenna and the new circuitry. Additionally, packaging considerations would need to be taken into account as this design would approach a more commercial aspect. The antenna would need to be re-characterized and the performance of the Tx/Rx measured. This could include using the transmitter and receiver as a pair or separately with an off-chip antenna.

References

[1] G. Falciasecca and B. Valotti, "Guglielmo Marconi: the Pioneer of Wireless Communications," in *the 39th European Microwave Conference*, Rome, 2009, pp. 544-546.

[2] Nobel Foundation. (2010, Jun.) Nobelprize.org. [Online]. http://nobelprize.org/nobel_prizes/physics/laureates/

[3] Federal Communications Commission, "Revision of Part 15 of the Commission's Rules Regarding Ultra-Wideband Transmission Systems," FCC, Washington D.C., First Report and Order 02-48, 2002.

[4] M. Z. Win, D. Dardari, A. F. Molisch, W. Wiesbeck, and J. Zhang, "History and Applications of UWB," *Proceedings of the IEEE*, vol. 97, no. 2, pp. 198-204, Feb. 2009.

[5] Federal Communications Commision, "Title 47 of the Code of Federal Regulations," FCC Part 15, Radio Frequency Devices, Subpart F 15.500, 2009.

[6] Industry Canada, "Devices Using Ultra-Wideband (UWB) Technology," Spectrum Management and Telecommunications Radio Standards Specification RSS-220, March 2009.

[7] W. Wiesbeck and G. Adamiuk, "Antennas for UWB-Systems," in *Antennas, 2007. INICA '07. 2nd International ITG Conference on*, Munich, March 2007, pp. 67-71.

[8] W. Wiesbeck, G. Adamiuk, and C. Sturm, "Basic Properties and Design Principles of UWB Antennas," *Proceedings of the IEEE*, vol. 97, no. 2, pp. 372-385, Feb. 2009.

[9] Zhi Ning Chen, "UWB Antennas: Design and Application," in *6th International Conference on Information, Communications & Signal Processing*, Singapore, 2007, pp. 1-5.

[10] J. S. Kilby, "The Integrated Circuit's Early History," *Proceedings of the IEEE*, vol. 88, no. 1, pp. 109-111, Jan. 2000.

[11] I. Young, "A History of the Continuously Innovative Analog Integrated Circuit,"

Solid-State Circuits Newsletter, IEEE, vol. 12, no. 4, pp. 52-57, Fall 2007.

[12] T. H. Lee, "The (Pre-) History of the Integrated Circuit: A Random Walk," *Solid-State Circuits Newsletter, IEEE*, vol. 12, no. 2, pp. 16-22, Spring 2007.

[13] K. K. O, et al., "On-Chip Antennas in Silicon ICs and Their Application," *IEEE Transactions on Electron Devices*, vol. 52, no. 7, pp. 1312-1323, Jul. 2005.

[14] W. L. Stutzman and G. A. Thiele, *Antenna Theory and Design*, 1st ed. New York, USA: John Wiley & Sons, Inc., 1981.

[15] "IEEE Standard Definitions of Terms for Antennas.," IEEE Std 145-1993, vol., no., pp.i, 1993. doi: 10.1109/IEEESTD.1993.119664.

[16] D. M. Pozar, *Microwave Engineering*, 2nd ed., C. Robey, Ed. New York, USA: John Wiley & Sons, 1998.

[17] P. Popovski, H. Yomo, and R. Prasad, "Strategies For Adaptive Frequency Hopping in the Unlicensed Bands," *IEEE Wireless Communications*, vol. 13, no. 6, pp. 60-67, Dec. 2006.

[18] W. Y. Zou and Y. Wu, "COFDM: An Overview," *IEEE Transactions on Broadcasting*, vol. 41, no. 1, pp. 1-8, Mar. 1995.

[19] Hiroshi Iwai, "RF CMOS Technology," in *Radio Science Conference, 2004. Proceedings. 2004 Asia-Pacific*, 24 - 27 August 2004, pp. 296-298.

[20] Y. Cheng, "An Overview of Device Behavior and Modeling of CMOS Technology for RF IC Design," in *The 11th IEEE International Symposium on Electron Devices for Microwave and Optoelectronic Applications, 2003. EDMO 2003.*, 17 - 18 November 2003, pp. 109-114.

[21] Xiaoling Guo, Ran Li, and K. K. O, "Design Guidlines for Reducing the Impact of Metal Interference Structures on the Performance of On-chip Antennas," in *Antennas and Propagation Society International Symposium, 2003. IEEE* , 2003, pp. 606-609.

[22] F. Gutierrez, S. Agarwal, K. Parrish, and T. S. Rappaport, "On-Chip Integrated Antenna Structures in CMOS for 60 GHz WPAN Systems," *IEEE Journal on Selected Areas in Communications*, vol. 27, no. 8, pp. 1367-1378, Oct. 2009.

[23] M. Pons, F. Touati, and P. Senn, "Study of On-Chip Integrated Antennas Using Standard Silicon Technology for Short Distance Communications," in *The European Conference on Wireless Technology, 2005.*, Paris, 2005, pp. 253-256.

[24] A. Shamim, et al., "Silicon Differential Antenna/Inductor for Short Range Wireless Communication Applications," in *Canadian Conference on Electrical and Computer Engineering, 2006. CCECE '06.* , Ottawa, ON, 2006, pp. 94-97.

[25] L. Fragomeni, F. Zito, F. G. Della Corte, F. Aquilino, and M. Merenda, "CMOS Fully Integrated 2.5GHz Active RFID Tag withOn-Chip Antenna," in *MELECON 2010 - 2010 15th IEEE Mediterranean Electrotechnical Conference*, Valletta, 2010, pp. 922-926.

[26] J. J. H. Wang, "The Physical Foundation, Developmental History, and Ultra-wideband Performance of SMM (Spiral-Mode Microstrip) Antennas," in *2005 IEEE Antennas and Propagation Society International Symposium*, July 2005, pp. 586-589vol3A.

[27] J. Liang, C. C. Chiau, X. Chen, and C. G. Parini, "Study of a Printed Circular Disc Monopole Antenna for UWB Systems," *IEEE Transactions on Antennas and Propagation*, vol. 53, no. 11, pp. 3500-3504, Nov. 2005.

[28] Y. Lu, Y. Huang, Y. C. Shen, and H. T. Chattha, "A Further Study of Planar UWB Monopole Antennas," in *Antennas & Propagation Conference, 2009. LAPC 2009.*, Loughborough , November 2009, pp. 353-356.

[29] Z. N. Chen, et al., "Planar Antennas," *IEEE Microwave Magazine*, vol. 7, no. 6, pp. 63-73, Dec. 2006.

[30] H. G. Schantz, "Bottom Fed Planar Elliptical UWB Antennas," in *2003 IEEE Conference on Ultra Wideband Systems and Technologies*, November 2003, pp. 219-223.

[31] M. Mao and C. Nguyen, "An Ultra-Wideband Uniplanar Antenna for UWB Systems," in *2008 International Radar Symposium*, Wroclaw, 2008, pp. 1-3.

[32] L. Tianming, R. Yuping, and N. Zhongxia, "Analysis and Design of UWB Vivaldi Antenna," in *2007 International Symposium on Microwave, Antenna, Propagation and EMC Technologies for Wireless Communications*, Hangzhou, 2007, pp. 579-581.

[33] V. Rumsey, "Frequency Independent Antennas," in *IRE International Convention Record*, 1957, pp. 114-118.

[34] G. Lu, P. Spasojevic, and L. Greenstein, "Antenna and Pulse Designs for Meeting UWB spectrum Density Requirements," in *2003 IEEE Conference on Ultra Wideband Systems and Technologies*, 2003, pp. 162-166.

[35] J. A. Gonzalez, T. M. Babij, and K. Siwiak, "Diamond Dipole Antenna Optimization Using a Genetic Algorithm/Finite Difference Time Domain Hybrid Technique.," in *IEEE 10th Annual Wireless and Microwave Technology Conference, 2009. WAMICON '09.*, Clearwater, FL, 2009, pp. 1-2.

[36] Y. Mushiake, "Self-Complementary Antennas," *IEEE Antennas and Propagation Magazine*, vol. 34, no. 6, pp. 23-29, Dec. 1992.

[37] H. A. Wheeler, "Fundamental Limitations of Small Antennas," *Proceedings of the IRE*, vol. 35, no. 12, pp. 1479-1484, Dec. 1947.

[38] L. J. Chu, "Physical Limitations of Omni-Directional Antennas," *Journal of Applied Physics*, vol. 19, no. 12, pp. 1163-1175, Dec. 1948.

[39] A. K. Skrivervik, J. .-F. Zurcher, O. Staub, and J. R. Mosig, "PCS Antenna Design: The Challenge of Miniaturization," *IEEE Antennas and Propagation Magazine*, vol. 43, no. 4, pp. 12-27, Aug. 2001.

[40] S. E. Sussman-Fort and R. M. Rudish, "Non-Foster Impedance Matching of Electrically-Small Antennas," *IEEE Transactions on Antennas and Propagation*, vol. 57, no. 8, pp. 2230-2241, Aug. 2009.

[41] J. S. McLean, "The Radiative Properties of Electrically-Small Antennas," in *IEEE International Symposium on Electromagnetic Compatibility, 1994. Symposium Record. Compatibility in the Loop.*, Chicago, 1994, pp. 320-324.

[42] Y.-j. Kim, J.-k. Kim, J.-h. Kim, H.-y. Kim, and H.-m. Lee, "Negative Permeability Metamaterial Structure Based Electrically Small Loop Antenna," *10th International Conference on Advanced Communication Technology, 2008. ICACT 2008.*, vol. 1, pp. 769-773, Feb. 2008.

[43] Z. N. Chen, T. S. P. See, and X. Qing, "Small Ground-independent Planar UWB Antenna," in *IEEE Antennas and Propagation Society International Symposium 2006*, Albuquerque, NM, 2006, pp. 1635-1638.

[44] M. Klemm and G. Troster, "Integration of Electrically Small UWB Antennas for Body-Worn Sensor Applications," in *Wideband and Multi-band Antennas and Arrays, 2005. IEE (Ref. No. 2005/11059)* , 2005, pp. 141-145.

[45] R. Saleem and A. K. Browne, "Electrically Small Band-Notch Reflected Inverse Parabolic Step Sequence Ultra Wideband Antenna," in *2010 Proceedings of the Fourth European Conference on Antennas and Propagation (EuCAP)*, Barcelona, Spain , 2010, pp. 1-3.

[46] M. Ikebe, et al., "A 3.1–10.6 GHz RF CMOS Circuits Monolithically Integrated with Dipole Antenna," in *16th IEEE International Conference on Electronics, Circuits, and Systems, 2009. ICECS 2009.* , Yasmine Hammamet, December 2009, pp. 17-20.

[47] K. Takahagi, M. Ohno, M. Ikebe, and E. Sano, "Ultra-Wideband Silicon On-Chip Antenna with Artificial Dielectric Layer," in *International Symposium on Intelligent Signal Processing and Communication Systems, 2009. ISPACS 2009.*, Kanazawa, 2009, pp. 81-84.

[48] K. T. Ansari and C. Plett, "A Low Power Ultra-Wideband CMOS LNA for 3.1-10.6-GHz Wireless Receivers," in *Proceedings of 2010 IEEE International Symposium on Circuits and Systems (ISCAS)*, Paris, France, 2010, pp. 209-212.

[49] O. Salehi-Abari and C. Plett, "A Differential 5th Derivative Gaussian Pulse Generator for UWB Transceivers," in *Proceedings of 2010 IEEE International Symposium on Circuits and Systems (ISCAS)*, Paris, France, 2010, pp. 1089-1092.

[50] Ansys Inc. (2010) Ansoft - HFSS. [Online]. http://www.ansoft.com/products/hf/hfss/